Discrete and Continuous Dynamical Systems - Series B
doi:10.3934/dcdsb.2024146

NETWORKS OF PIECEWISE SMOOTH FILIPPOV SYSTEMS AND STABILITY OF SYNCHRONOUS PERIODIC ORBITS

Luca Dieci*[1], Cinzia Elia[2] and Luciano Lopez[2]
[1]School of Mathematics, Georgia Tech, Atlanta, GA 30332, U.S.A.
[2]Dipartimento di Matematica, Univ. of Bari, I-70100, Bari, Italy

Abstract. In this work, we considered networks of piecewise- smooth (PWS) differential equations of Filippov type, which we call PWS Filippov networks, whose single agent has an asymptotically stable periodic orbit, that becomes a synchronous periodic orbit for the network. We investigated the stability of the synchronous periodic orbit by using both the master stability function (MSF) tool and direct integration of the "regularized network", that is the network obtained by replacing the PWS differential agents by a suitable smooth approximation. We present several new results on the class of Filippov PWS networks that depend on several coupling matrices. (i) We studied an associated MSF that depends on several coupling strengths, and (ii) we employed a one-parameter family of regularized networks, observed that it is equivalent to a network of regularized agents, and showed that its solutions converge to the solutions of the PWS network as the regularization parameter goes to 0. Furthermore, when the synchronous periodic orbit is asymptotically stable and does not slide on the discontinuity surface, (iii) we showed that the regularized network has an asymptotically stable synchronous periodic orbit as well. Finally, (iv) we performed detailed numerical experiments on two different problems, highlighting specific characteristics of PWS networks with a synchronous periodic orbit. More specifically, (a) first, we considered the case of a network of planar PWS oscillators, with the network depending on two different coupling parameters and the synchronous periodic trajectory undergoing sliding regime; then, (b) we considered a network where the single agent obeys 3D PWS dynamics with the synchronous periodic orbit undergoing repeated crossing of two distinct discontinuity planes. On our two problems, we also showed how the convergence behavior to the synchronous subspace can be used to obtain the same rates of attractivity predicted by the MSF.

1. **Motivation, background, and notations.** In this work, we consider networks of agents that, when uncoupled, satisfy identical piecewise smooth (PWS) differential systems of Filippov type having a stable periodic orbit and that are coupled together through linear anti-symmetric couplings. We call these *piecewise smooth (PWS) networks*.

2020 *Mathematics Subject Classification.* Primary: 34A36, 34D06; Secondary: 34D08.
Key words and phrases. Piecewise smooth networks, synchronization, Filippov, master stability function, periodic orbit, Floquet mutlipliers.
This work has been partially supported by the GNCS-Indam group and the PRIN2017 [2017E844SL].

*Corresponding author: Luca Dieci.

In [13, Definition 23, Theorem 21 and Remark 22], we derived the expression of the monodromy matrix along a synchronous periodic orbit of a PWS network and generalized the master stability function (MSF) of Pecora and Carroll (see [27]) to PWS networks. We also performed numerical experiments on a network of PWS mechanical oscillators studied in [21, 20], by computing the MSF for a network of N agents and for a prescribed interval of parameter values (see [13, Figure 4]). Finally, in [13], we further verified the correctness of our results by direct integration in forward time of a PWS network with 2 agents and we observed perfect agreement in having synchronization, or lack thereof, of the numerical solution with the parameter values predicted by the MSF.

The MSF for a PWS system of the type considered in this work was essentially derived in the recent work [13] where two of us considered precisely the class of Filippov systems tackled in the present work, with solutions exhibiting a combination of sliding and crossing behaviors. Earlier works of Coombes and coauthors [9, 8] considered the MSF for piecewise linear systems, and the work [23] derived the MSF for the class of impacting PWS networks, in which the state but not the vector field changes at so-called reset points. Of course, in order to infer global asymptotic stability of the synchronous solution, there are alternatives to the MSF, essentially based on logarithmic norms arguments; see the works by Coraggio and coworkers in [11, 10], where σ-QUADness of the single agent vector field was employed. An advantage of using the MSF in our context is that it only necessitates knowledge of the behavior of the periodic orbit of (4) and appropriate linearized analysis (see below).

Unfortunately, direct integration of a PWS network with more than 2 agents is at best cumbersome (if not plainly out of reach), since it requires the evaluation of $2^N + 2\sum_{k=1}^{N} \binom{N}{k}$ vector fields at the intersection of N discontinuity hyperplanes, and one must take into account all these vector fields at each step when computing the numerical solution. In the present paper, we avoid this issue by introducing a **one-parameter** family of regularized vector fields, where these new vector fields are suitable smooth approximations to the original PWS problem; we consider the resulting regularized, smooth network. Our main theoretical results will show that the solutions of this regularized network converge to solutions of the PWS network; see Theorem 2.8. Moreover, for an asymptotically stable synchronous crossing periodic orbit $\boldsymbol{x}_s(t)$ (see Section 2), we also show that the monodromy matrix along the synchronous periodic orbit of the regularized network converges to the monodromy matrix along $\boldsymbol{x}_s(t)$. Finally, we also obtain new results for the class of PWS networks considered, showing that the convergence behavior to the synchronous subspace can be used to obtain the same rates of attractivity given by the MSF.

A plan of our paper is as follows. Hereafter, we give the basic PWS model considered here, set up the notations, and discuss the MSF for smooth systems. In Section 2, we give details on the MSF for PWS networks, give and justify the regularized system considered here, and show the aforementioned convergence results. Finally, in Section 3, we discuss in detail two numerical examples to validate our theoretical results and further give a new algorithm to show how the convergence behavior to the synchronous subspace can be used to obtain the same rates of attractivity predicted by the MSF.

Notation 1. Boldface will be used for vectors throughout this work. We will write $\boldsymbol{x}, \boldsymbol{y}, \boldsymbol{z}$, for vectors in $\mathbb{R}^n$, or in $\mathbb{R}^N$, or in $\mathbb{R}^{nN}$. Similarly, $\boldsymbol{e}_1, \boldsymbol{e}_2, \dots$, will indicate the unit vectors in $\mathbb{R}^n$, $\mathbb{R}^N$ or $\mathbb{R}^{nN}$. The i-th component of a vector $\boldsymbol{x}$ is $\boldsymbol{e}_i^T\boldsymbol{x}$ and will be indicated with x_i.

1.1. **Our model.** Our model is the following system

$$\dot{\boldsymbol{x}}_i = \boldsymbol{f}(\boldsymbol{x}_i) + \sum_{k=1}^{p} \sigma_k \sum_{j=1}^{N} a_{ij} E_k(\boldsymbol{x}_j - \boldsymbol{x}_i), \;\; i = 1, \dots, N, \tag{1}$$

where each $\boldsymbol{x}_i \in \mathbb{R}^n$, $A = (a_{ij})_{i,j=1:N}$ is the adjacency matrix of the network graph, which we will assume to be connected, and E_k's are coupling matrices in $\mathbb{R}^{n\times n}$ with respective coupling strengths $\sigma_k > 0$, $k = 1, \dots, p$. Recall that the negative of the graph Laplacian is the matrix $L = L^T \in \mathbb{R}^{N\times N}$ given by $L_{ij} = a_{ij}$, for $i \neq j$ and $L_{ii} = -\sum_j a_{ij}$, $i, j = 1, \dots, N$. Obviously, 0 is an eigenvalue of L, and since the graph is connected, 0 is a simple eigenvalue of L.

Let $\boldsymbol{x} = \begin{bmatrix} \boldsymbol{x}_1 \\ \vdots \\ \boldsymbol{x}_N \end{bmatrix} \in \mathbb{R}^{nN}$, $\boldsymbol{F}(\boldsymbol{x}) = \begin{bmatrix} \boldsymbol{f}(\boldsymbol{x}_1) \\ \vdots \\ \boldsymbol{f}(\boldsymbol{x}_N) \end{bmatrix}$, L be the (negative of the) graph Laplacian, and rewrite (1) as

$$\dot{\boldsymbol{x}} = \boldsymbol{F}(\boldsymbol{x}) + \sum_{k=1}^{p} \sigma_k M_k \boldsymbol{x}, \quad M_k = L \otimes E_k, \;\; k = 1, \dots, p\ . \tag{2}$$

We note that if $\boldsymbol{z} : \; t \in \mathbb{R} \to \boldsymbol{z}(t) \in \mathbb{R}^n$ is a T-periodic solution for the single agent equation $\dot{\boldsymbol{z}} = \boldsymbol{f}(\boldsymbol{z})$, then (2) always has the T-periodic solution $\boldsymbol{x}_1 = \boldsymbol{x}_2 = \cdots = \boldsymbol{x}_N = \boldsymbol{z}$. This is called *synchronous solution* and we denote it as $\boldsymbol{x}_s$. With

$$\mathcal{S} = \{\boldsymbol{x} \in \mathbb{R}^{nN} : \; \boldsymbol{x}_1 = \boldsymbol{x}_2 = \cdots = \boldsymbol{x}_N \;, \boldsymbol{x}_j \in \mathbb{R}^n, \; j = 1, \dots, N\} \tag{3}$$

we indicate the *synchronous subspace*. We denote by $B_d(\boldsymbol{x}_s)$ the d-tube of $\boldsymbol{x}_s$:

$$B_d(\boldsymbol{x}_s) := \{\boldsymbol{x} \in \mathbb{R}^{nN} \;\; : \;\; \|\boldsymbol{x} - \boldsymbol{x}_s(t)\| < d, \qquad t \in [0, T]\}.$$

Therefore, if $\boldsymbol{z}$ is an asymptotically stable solution for the single agent, it follows that there always exists a $d > 0$ such that all solutions in $B_d(\boldsymbol{x}_s) \cap \mathcal{S}$ converge to $\boldsymbol{x}_s(t)$. Therefore, in order to ascertain the asymptotic stability of $\boldsymbol{x}_s$, one needs to study the asymptotic behavior of solutions of (2) transversal to $\mathcal{S}$.

Remark 1.1. The model (1) is similar to the so-called multiplex, or multilayer networks, extensively studied in the literature on smooth networks: when the single agent satisfies a smooth differential equation. For example, see [29, 12, 28, 26, 32, 6, 5, 7, 34] for a sample of relevant references, relative to just two-layer networks. There are some differences, however, between our model and these other works. Namely, in the cited works on multiplex networks, the authors typically consider different Laplacian matrices, whereas we only consider one Laplacian matrix. If the authors of these cited works want to achieve the standard dimensional reduction afforded as when using the master stability function tool for a standard one-layer network, then they need to restrict to commuting Laplacian matrices, which renders all of them simultaneously diagonalizable (e.g., see [32]); an exception is [34], where the author considers a directed graph, hence not necessarily symmetric Laplacian matrices but restrict to the commuting case and, therefore, is able to simultaneously triangularize all of the Laplacian matrices. Our interest, on the other hand, motivated by networks of second-order oscillators (see Example 1.2), is to have just one Laplacian matrix but several different coupling terms among the components of each agent, hence the model (1). Moreover, we are interested in the case in which the single agent obeys a PWS system of differential equations (see below). To the best of our knowledge, this case has not been treated before in the multilayer literature.

As previously remarked, in (1), we are interested in studying a network of N agents $\boldsymbol{x}_i \in \mathbb{R}^n$ satisfying a PWS system of Filippov type (also called *bimodal*). That is, each agent satisfies the system

$$\dot{\boldsymbol{z}} = \boldsymbol{f}(\boldsymbol{z}) = \begin{cases} \boldsymbol{f}^+(\boldsymbol{z}), & \text{if} \quad \boldsymbol{z} \in R^+ \equiv \{\boldsymbol{z} \in \mathbb{R}^n : \ h(\boldsymbol{z}) > 0\}, \\ \boldsymbol{f}^-(\boldsymbol{z}), & \text{if} \quad \boldsymbol{z} \in R^- \equiv \{\boldsymbol{z} \in \mathbb{R}^n : \ h(\boldsymbol{z}) < 0\}, \end{cases} \tag{4}$$

with $h : \mathbb{R}^n \to \mathbb{R}$ defining the discontinuity surface. In this work, we restrict consideration to the case when $h(\boldsymbol{z})$ is a hyperplane, which (without loss of generality) we will take to be $\boldsymbol{e}_1^T \boldsymbol{z} - b = 0$, unless otherwise stated. We denote by Σ the zero set of $h(\boldsymbol{z})$ in $\mathbb{R}^n$:

$$\Sigma = \{\boldsymbol{z} \in \mathbb{R}^n \ : \ \boldsymbol{e}_1^T \boldsymbol{z} - b = 0\} \quad \text{and note that} \quad \nabla h(\cdot) = \boldsymbol{e}_1 \ . \tag{5}$$

Obviously, the differential equation (4) is not defined when $\boldsymbol{z} \in \Sigma$, and we consider the extension of Filippov to points on Σ; see [19].

To recall, we say that a point $\widehat{\boldsymbol{z}} \in \Sigma$ is a *transversal crossing point* if

$$(\nabla h(\widehat{\boldsymbol{z}})^T \boldsymbol{f}^-(\widehat{\boldsymbol{z}}))(\nabla h(\widehat{\boldsymbol{z}})^T \boldsymbol{f}^+(\widehat{\boldsymbol{z}})) > 0, \tag{6}$$

see point s_1 in Figure 1, it is an *attractive sliding point* if

$$\nabla h(\widehat{\boldsymbol{z}})^T \boldsymbol{f}^-(\widehat{\boldsymbol{z}}) > 0, \quad \nabla h(\widehat{\boldsymbol{z}})^T f^+(\widehat{\boldsymbol{z}}) < 0, \tag{7}$$

see point s_2 in Figure 1, and a *repulsive sliding point* if

$$\nabla h(\widehat{\boldsymbol{z}})^T \boldsymbol{f}^-(\widehat{\boldsymbol{z}}) < 0, \quad \nabla h(\widehat{\boldsymbol{z}})^T f^+(\widehat{\boldsymbol{z}}) > 0.$$

The case of repulsive sliding is ill-posed since at a repulsive sliding point one can either remain on Σ or leave it to enter in either R^+ or R^-; for this reason, hereafter we will not consider repulsive sliding.

On Σ, sliding will be assumed to take place in the sense of Filippov. That is, on Σ, *sliding motion* takes place with the vector field given by $\boldsymbol{f}_\Sigma$ below:

$$\dot{\boldsymbol{z}} = \boldsymbol{f}_\Sigma(\boldsymbol{z}), \quad \boldsymbol{f}_\Sigma(\boldsymbol{z}) = (1-\alpha)\boldsymbol{f}^-(\boldsymbol{z}) + \alpha \boldsymbol{f}^+(\boldsymbol{z}) \ , \quad \alpha(\boldsymbol{z}) = \frac{\nabla h^T \boldsymbol{f}^-(\boldsymbol{z})}{\nabla h^T (\boldsymbol{f}^- - \boldsymbol{f}^+)(\boldsymbol{z})} \ . \tag{8}$$

Finally, a point $\widehat{\boldsymbol{z}} \in \Sigma$ is called *tangential exit point into* R^- if a trajectory $\boldsymbol{z}(t)$ sliding on Σ reaches $\widehat{\boldsymbol{z}}$ at some value $\widehat{t}$, that is $\widehat{\boldsymbol{z}} = \boldsymbol{z}(\widehat{t})$, and there it holds that

$$\begin{aligned} &\nabla h(\widehat{\boldsymbol{z}})^T \boldsymbol{f}^-(\widehat{\boldsymbol{z}}) = 0, \quad \nabla h(\widehat{\boldsymbol{z}})^T \boldsymbol{f}^+(\widehat{\boldsymbol{z}}) < 0, \\ &\left[\frac{d}{dt} \left(\nabla h(\boldsymbol{z}(t))^T \boldsymbol{f}^-(\boldsymbol{z}(t)) \right) \right]_{t=\widehat{t}} < 0, \end{aligned} \tag{9}$$

see the point s_3 in Figure 1, and similarly for a tangential exit point into R^+. All together, transversal crossings of Σ, transversal entries on Σ, and tangential exits from Σ are called *generic events* or simply *events*. We will henceforth assume that all points on Σ reached by a solution of (4) are either parts of an attractive sliding trajectory or generic events.

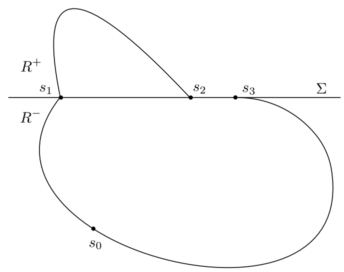

FIGURE 1. Model periodic orbit of (4) with generic events.

Example 1.2. The simplest (and most often studied) case of (2) is when $p = 1$, meaning that there is only one coupling term E. However, we favor the writing with several coupling terms to accommodate the distinct roles played by coupling different components of the different agents. To exemplify our interest in the more general model (1), consider a chain of identical second-order oscillators rewritten in first-order form $\begin{bmatrix} x \\ \dot{x} \end{bmatrix}$, coupled not just by position but also through a viscous coupling term (e.g., this is the case considered in [18], [24], and [2]). That is, we have

$$\begin{cases} \dot{\boldsymbol{x}}_1 &= \boldsymbol{f}(\boldsymbol{x}_1) + \left[\sigma_1 \begin{pmatrix} 0 & 0 \\ 1 & 0 \end{pmatrix} + \sigma_2 \begin{pmatrix} 0 & 0 \\ 0 & 1 \end{pmatrix}\right] (\boldsymbol{x}_2 - \boldsymbol{x}_1) \\ \dot{\boldsymbol{x}}_i &= \boldsymbol{f}(\boldsymbol{x}_i) + \left[\sigma_1 \begin{pmatrix} 0 & 0 \\ 1 & 0 \end{pmatrix} + \sigma_2 \begin{pmatrix} 0 & 0 \\ 0 & 1 \end{pmatrix}\right] (\boldsymbol{x}_{i+1} - 2\boldsymbol{x}_i + \boldsymbol{x}_{i-1}) \\ & \quad i = 2, \dots, N-1 \\ \dot{\boldsymbol{x}}_N &= \boldsymbol{f}(\boldsymbol{x}_N) + \left[\sigma_1 \begin{pmatrix} 0 & 0 \\ 1 & 0 \end{pmatrix} + \sigma_2 \begin{pmatrix} 0 & 0 \\ 0 & 1 \end{pmatrix}\right] (\boldsymbol{x}_{N-1} - \boldsymbol{x}_N). \end{cases} \tag{10}$$

In (10), the graph has the standard nearest neighbor structure, which gives the negative Laplacian

$$L = \begin{bmatrix} -1 & 1 & & & \\ 1 & -2 & 1 & & \\ & \ddots & \ddots & \ddots & \\ & & 1 & -2 & 1 \\ & & & 1 & -1 \end{bmatrix} \tag{11}$$

The coupling matrices E_1, E_2 are $E_1 = \begin{pmatrix} 0 & 0 \\ 1 & 0 \end{pmatrix}$, $E_2 = \begin{pmatrix} 0 & 0 \\ 0 & 1 \end{pmatrix}$.

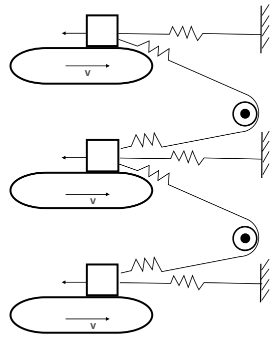

FIGURE 2. Stick slip coupled oscillators.

Furthermore, in this work, we will study the case of piecewise smooth oscillators with dry friction term of the type studied in [13, 21, 20] (see Section 3.1). In (10), we have

$$\boldsymbol{f}(\boldsymbol{z}) = \boldsymbol{f}^{\pm}(\boldsymbol{z}) = \begin{bmatrix} x_2 \\ -x_1 \mp \frac{1}{1 \pm \gamma(x_2 - v)} \end{bmatrix} \tag{12}$$

where one takes $\boldsymbol{f}^+$ if $x_2 - v > 0$ and $\boldsymbol{f}^-$ if $x_2 - v < 0$ (there is a sliding motion when $x_2 = v$). An illustration of the case of 3 coupled oscillators of the type in (12), coupled through positions and velocity, is in Figure 2.

1.2. **MSF for several coupling matrices: Smooth case.** One of our goals in this work is to study the stability of a synchronous periodic solution for a network given by (10), via the master stability function tool. Ever since the work of Pecora and Carroll, [27], this has been the most widely adopted tool to study the stability of a synchronous solution of a network, with respect to perturbations transversal to $\mathcal{S}$. For completeness, below we give the MSF tool for the case of several coupling matrices by a simple extension of the MSF for a single coupling matrix, in the case where $\boldsymbol{f}$ and $\boldsymbol{F}$ in (2) are smooth. Then, in the next section, we will present it for the PWS case.

Let $\boldsymbol{z}(t)$ be a periodic solution of period T of the single agent dynamics:

$$\dot{\boldsymbol{z}} = \boldsymbol{f}(\boldsymbol{z}) \longrightarrow \boldsymbol{z}(t+T) = \boldsymbol{z}(t),$$

where $\boldsymbol{f}$ is a smooth vector field, and let $\boldsymbol{x}_s(t) = \begin{bmatrix} \boldsymbol{z}(t) \\ \vdots \\ \boldsymbol{z}(t) \end{bmatrix}$ be the synchronous T-periodic solution of the network, with $\boldsymbol{x}_s(t) \in \mathbb{R}^{nN}$ for all t. Since $\boldsymbol{f}$ in (1) is a smooth function, we linearize (2) about $\boldsymbol{x}_s$ and end up with the system for the first variation $\boldsymbol{y} = \begin{bmatrix} \boldsymbol{y}_1 \\ \vdots \\ \boldsymbol{y}_N \end{bmatrix}$:

$$\begin{aligned}\dot{\boldsymbol{y}} =& D\boldsymbol{F}(\boldsymbol{x}_s(t))\boldsymbol{y} + \sum_{k=1}^{p} \sigma_k M_k \boldsymbol{y} \equiv \begin{pmatrix} D\boldsymbol{f}(\boldsymbol{z}(t)) & & \\ & \ddots & \\ & & D\boldsymbol{f}(\boldsymbol{z}(t)) \end{pmatrix} \boldsymbol{y} + \sum_{k=1}^{p} \sigma_k M_k \boldsymbol{y} \\ =& (I_N \otimes D\boldsymbol{f}(\boldsymbol{z}(t)))\boldsymbol{y} + \sum_{k=1}^{p} \sigma_k M_k \boldsymbol{y} \ , \quad M_k = L \otimes E_k \ .\end{aligned}$$

Now, recall that $L = L^T$ and let U be the orthogonal matrix of eigenvectors of L: $L = U\Lambda U^T$, where Λ is the diagonal matrix of eigenvalues ordered in decreasing way: $0 = \lambda_1 > \lambda_2 \geq \cdots \geq \lambda_N$. Further, let V be either the identity I_n or a matrix (if it exists) that diagonalizes all E_k's, namely if all E_k's commute and are diagonalizable, and set $J_k = V^{-1}E_kV$, $k = 1, \dots, p$. If the E_k's are not simultaneously diagonalizable, then $V = I_n$ and $J_k = E_k$. With this, we can write

$$M_k = L \otimes E_k = U\Lambda U^T \otimes VJ_kV^{-1} = (U \otimes V)(\Lambda \otimes J_k)(U \otimes V)^{-1} \ .$$

Moreover $(U \otimes V)(I \otimes D\boldsymbol{f}(\boldsymbol{x}))(U \otimes V)^{-1} = (I \otimes VD\boldsymbol{f}(\boldsymbol{x})V^{-1})$. Let $A(t) = VD\boldsymbol{f}(\boldsymbol{z}(t))V^{-1}$, then by letting $\boldsymbol{w} = (U \otimes V)^{-1}\boldsymbol{y}$, we get

$$\begin{aligned}\dot{\boldsymbol{w}} &= (I_N \otimes A(t))\boldsymbol{w} + \sum_{k=1}^{p} \sigma_k \Lambda \otimes J_k \boldsymbol{w} \\ &= \begin{pmatrix} A(t) + \lambda_1 \sum_k \sigma_k J_k & & \\ & \ddots & \\ & & A(t) + \lambda_N \sum_k \sigma_k J_k \end{pmatrix} \boldsymbol{w}, \end{aligned} \tag{13}$$

with $J_k = E_k$ if the E_k's are not simultaneously diagonalizable. Given that the synchronous solution $\boldsymbol{x}_s$ is periodic of period T, the coefficient matrix $A(t)$ is T-periodic, and so is the linear system (13), hence we can study the stability of the synchronous solution via Floquet theory.

Definition 1.3. From (13), we define the MSF to be the largest Lyapunov exponent (real part of the logarithms of the Floquet multipliers) of the $N-1$ systems with coefficient matrices $A(t) + \lambda_j \sum_k^p \sigma_k J_k$, $j = 2, \dots, N$. The synchronous orbit is *transversally stable* for those values of σ_k, $k = 1, \dots, p$, (if any) for which the MSF is negative.

Clearly, we can define the MSF directly from the multipliers, that is from the eigenvalues of the monodromy matrices of the $N-1$ systems with coefficient matrices $A(t)+\lambda_j \sum_k^p \sigma_k J_k$, $j = 2, \dots, N$. In this case, the synchronous orbit is transversally stable for those values of σ_k, $k = 1, \dots, p$, (if any) for which the multipliers are less than 1 (in absolute value).

Note that the Floquet multipliers, hence the MSF, depend on the p parameters $\sigma_1, \dots, \sigma_p$. This allows for treating different couplings at different strength. For example, in an application like that of Example 1.2, the viscous coupling coefficients might be an order of magnitude smaller than the elastic coupling strength.

Example 1.4. Consider the case of (11) and recall Example 1.2. Then, for the eigenvectors U and eigenvalues Λ of L, we have

$$\lambda_1 = 0 \ , \ \lambda_j = -4\sin^2\left(\frac{(j-1)\pi}{2N}\right) = -2 + 2\cos\left(\frac{(j-1)\pi}{N}\right), j = 2, \dots, N \ ,$$

$$U_{i1} = \sqrt{\frac{1}{N}} \ , \ \ U_{ij} = \sqrt{\frac{2}{N}}\cos\left(\frac{(i-0.5)(j-1)\pi}{N}\right) \ , \ \ i, j = 1, \dots, N \ .$$

Furthermore, since $E_1 = \begin{pmatrix} 0 & 0 \\ 1 & 0 \end{pmatrix}$, and $E_2 = \begin{pmatrix} 0 & 0 \\ 0 & 1 \end{pmatrix}$, we can take the matrix $V = I$ and keep $J_1 = E_1$ and $J_2 = E_2$.

2. **Piecewise smooth agents, the MSF, and regularization.**

Our interest is for when, in (1), the vector field $\boldsymbol{f}$ is piecewise smooth. That is, we study the following network of N agents $\boldsymbol{x}_i \in \mathbb{R}^n$ satisfying PWS dynamics of Filippov type:

$$\dot{\boldsymbol{x}} = \boldsymbol{F}(\boldsymbol{x}) + \sum_{k=1}^{p} \sigma_k M_k \boldsymbol{x}, \quad \boldsymbol{F}(\boldsymbol{x}) = \begin{pmatrix} \boldsymbol{f}^{\pm}(\boldsymbol{x}_1) \\ \vdots \\ \boldsymbol{f}^{\pm}(\boldsymbol{x}_n) \end{pmatrix} \ , \tag{14}$$

and for each agent, the vector field is defined in (4), with $h(\boldsymbol{x}_i) = 0$ given by $\boldsymbol{e}_1^T\boldsymbol{x} - b \equiv x_i^1 - b = 0$.

Notation 2. Σ denotes the discontinuity plane in $\mathbb{R}^n$ for a single agent, that is the set of $\boldsymbol{z} \in \mathbb{R}^n$ such that $h(\boldsymbol{z}) = 0$ with $h(\boldsymbol{z}) = \boldsymbol{e}_1^T\boldsymbol{z} - b = 0$. We let $h_i(\boldsymbol{x}) : \mathbb{R}^{nN} \to \mathbb{R}$ be defined as $h_i(\boldsymbol{x}) = h(\boldsymbol{x}_i)$. We denote by $\boldsymbol{\Sigma}_i$ the plane in $\mathbb{R}^{nN}$ defined as the zero set of $h_i(\boldsymbol{x})$, that is $\boldsymbol{\Sigma}_i = \{\boldsymbol{x} \in \mathbb{R}^{nN} \ : \ x_i^1 - b = 0\}$. Also, $\boldsymbol{\Sigma}$ will indicate the intersection of the $\boldsymbol{\Sigma}_i$'s: $\boldsymbol{\Sigma} = \cap_{i=1}^N \boldsymbol{\Sigma}_i$, while $\boldsymbol{\Sigma}_C$ is the intersection of the $\boldsymbol{\Sigma}_i$'s, for $i \in C$ and C is an index set (a subset of $\{1, 2, \dots, N\}$).

Thus, each $\boldsymbol{\Sigma}_i$ divides the phase space $\mathbb{R}^{nN}$ in two half-spaces (with corresponding vector fields), and altogether there will be 2^N regions, which we represent using a tree diagram with 2^N branches. The regions and the corresponding vector fields are numbered from 1 to 2^N following the branches of the tree, and to each region R_j, we assign the corresponding sequence of sign in the diagram tree.

Example. Below we illustrate with $N = 3$:

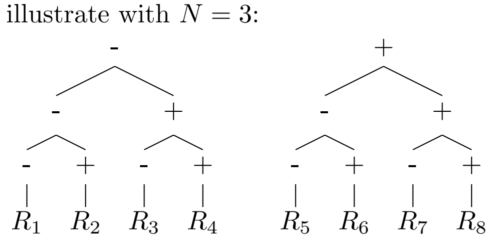

and we associate the sequence $(-, +, -)$ to R_3 .

In each region R_j, the vector field in (14) is $\boldsymbol{F}(\boldsymbol{x}) = \boldsymbol{F}_j(\boldsymbol{x}) = \begin{pmatrix} \boldsymbol{f}^{\pm}(\boldsymbol{x}_1) \\ \vdots \\ \boldsymbol{f}^{\pm}(\boldsymbol{x}_N) \end{pmatrix}$ for $j = 1, \dots 2^N$, where the $\pm$ signs are chosen in agreement with the corresponding signs of the h_j's. To illustrate, for the case $N = 3$, the vector field in R_3 is

$\boldsymbol{F}_3(\boldsymbol{x}) = \begin{pmatrix} \boldsymbol{f}^-(\boldsymbol{x}_1) \\ \boldsymbol{f}^+(\boldsymbol{x}_2) \\ \boldsymbol{f}^-(\boldsymbol{x}_3) \end{pmatrix}$. Finally, we define

$$\boldsymbol{G}_j(\boldsymbol{x}) = \boldsymbol{F}_j(\boldsymbol{x}) + \sum_{k=1}^{p} \sigma_k M_k \boldsymbol{x}, \quad j = 1, \dots, 2^N \ . \tag{15}$$

Again, we denote by $\boldsymbol{z}(t)$ an asymptotically stable periodic orbit of period T for the single agent and we also assume that the trajectory $\boldsymbol{z}(t)$ has a finite number of generic events and associated regimes of sliding; see Figure 1 for a typical situation. Let $\boldsymbol{x}_s(t) = \begin{bmatrix} \boldsymbol{z} \\ \vdots \\ \boldsymbol{z} \end{bmatrix}$ be the synchronous periodic orbit for the whole network. As for the smooth case, the asymptotic stability of $\boldsymbol{x}_s$ is not guaranteed in general. An algorithm that generalizes the MSF tool to the case of PWS Filippov systems is described in the next section.

2.1. **Master stability function, MSF, for the PWS case.** Assume (without loss of generality) that the initial condition $\boldsymbol{z}_0$ for the single agent dynamics is in one of the regions R^- or R^+. Call $t_0 = 0$ and let t_j, $j = 1, 2, \dots, M$ be the times where a generic event of $\boldsymbol{z}(t)$ occurs, and finally let $t_{M+1} = T$. To reiterate, the t_j's are the times where the single agent trajectory $\boldsymbol{z}_s(t)$ crosses Σ from one region $R^\pm$ to the other, or enters Σ (transversally) to slide on it, or exits Σ (tangentially) to enter in R^+ or R^-.

Extending the result of [13], and with the same arguments given there, the MSF is given by the largest Lyapunov exponent of the $(N-1)$ monodromy matrices $X_i(T) \in \mathbb{R}^{n \times n}$ given below, $i = 2, \dots, N$. With the notation $\eta_k = \sigma_k \lambda_i$, $k = 1, \dots, p$, and for each $i = 2, \dots, N$, these are given by (recall (4) and (8))

$$X_i(T) = \prod_{j=0}^{M} X_i(t_{j+1}, t_j) S_j, \quad \text{where} \quad \begin{cases} \frac{\partial}{\partial t} X_i(t, t_j) = & J_i(\boldsymbol{z}(t)) X_i(t, t_j) \\ X_i(t_j, t_j) = & I_n \end{cases}, \quad \text{and}$$

$$J_i(\boldsymbol{z}(t)) = \begin{cases} D\boldsymbol{f}^-(\boldsymbol{z}(t)) + \sum_{k=1}^{p} \eta_k E_k, & \boldsymbol{z}(t) \in R^-,\ t \in (t_j, t_{j+1}) \\ D\boldsymbol{f}^+(\boldsymbol{z}(t)) + \sum_{k=1}^{p} \eta_k E_k, & \boldsymbol{z}(t) \in R^+,\ t \in (t_j, t_{j+1}) \\ D\boldsymbol{f}_\Sigma(\boldsymbol{z}(t)) + \sum_{k=1}^{p} \eta_k \left(I + \frac{(\boldsymbol{f}^+ - \boldsymbol{f}^-)(\boldsymbol{z}(t)) \boldsymbol{e}_1^T}{\boldsymbol{e}_1^T (\boldsymbol{f}^- - \boldsymbol{f}^+)(\boldsymbol{z}(t))} \right) E_k, & \boldsymbol{z}(t) \in \Sigma,\ t \in (t_j, t_{j+1}) \end{cases} \tag{16}$$

and finally the so-called *saltation matrices* S_j's are given by

$$S_j = \begin{cases} I, & t_j = t_0 \text{ or } \boldsymbol{z}(t_j) \text{ tangential exit point} \\ S_{+,-} = I_n + \frac{(\boldsymbol{f}^- - \boldsymbol{f}^+)\boldsymbol{e}_1^T}{\boldsymbol{e}_1^T \boldsymbol{f}^+}\big|_{\boldsymbol{z}(t_j)}, & \boldsymbol{z}(t_j) \text{ crossing point from } R^+ \text{ to } R^- \\ S_{-,+} = I_n + \frac{(\boldsymbol{f}^+ - \boldsymbol{f}^-)\boldsymbol{e}_1^T}{\boldsymbol{e}_1^T \boldsymbol{f}^-}\big|_{\boldsymbol{z}(t_j)}, & \boldsymbol{z}(t_j) \text{ crossing point from } R^- \text{ to } R^+ \\ S_{+,\Sigma} = I_n + \frac{(\boldsymbol{f}_\Sigma - \boldsymbol{f}^+)\boldsymbol{e}_1^T}{\boldsymbol{e}_1^T \boldsymbol{f}^+}\big|_{\boldsymbol{z}(t_j)}, & \boldsymbol{z}(t_j) \text{ transversal entry point on } \Sigma \text{ from } R^+ \\ S_{-,\Sigma} = I_n + \frac{(\boldsymbol{f}_\Sigma - \boldsymbol{f}^-)\boldsymbol{e}_1^T}{\boldsymbol{e}_1^T \boldsymbol{f}^-}\big|_{\boldsymbol{z}(t_j)}, & \boldsymbol{z}(t_j) \text{ transversal entry point on } \Sigma \text{ from } R^-. \end{cases} \tag{17}$$

Remark 2.1. In the above expression for $J_i(\boldsymbol{z}(t))$, as well as in formula (17), and later below in (18) and thereafter, the term $\boldsymbol{e}_1^T$ arises because we are taking the discontinuity surface to be $h(\boldsymbol{z}) = \boldsymbol{e}_1^T \boldsymbol{z} - b$; see (5). For a different discontinuity manifold of the general form $h(\boldsymbol{z}) = 0$, we would need to replace $\boldsymbol{e}_1$ with $\nabla h(\cdot)$ in all of these formulas.

Remark 2.2. Naturally, the synchronous periodic orbit $\boldsymbol{x}_s$ is stable if all Floquet multipliers of all the systems (2.1) (for $i = 2, \dots, N$) are less than 1 in modulus. We note that the computation of the MSF is done with respect to the parameters $\eta_1, \dots, \eta_p$, in (16) (e.g., taking them in a certain range), and the eigenvalues of the (negative) Laplacian do not play any role. Only after determining the region of stability in the parameter space for $\eta_1, \dots, \eta_p$ we will assess whether or not it is possible to have an asymptotically stable synchronous periodic orbit for a prescribed network topology (hence for the eigenvalues associated to a specific choice of Laplacian L). That is, we first employ the MSF to find the region of stability $\mathcal{N}_1 \times \mathcal{N}_2 \dots \times \mathcal{N}_p$, $j = 1, \dots, p$, i.e, the set such that $\boldsymbol{x}_s$ is asymptotically stable (or stable in finite time), for $\eta_j \in \mathcal{N}_j$, $j = 1, \dots p$. Then, for a given topology, and hence a given L, we establish whether there are values of $\sigma_1, \dots, \sigma_p$, in (14), such that for all $i = 2, \dots, N$, $\sigma_j \lambda_i \in \mathcal{N}_j$, where λ_i's denote the eigenvalues of L. See Section 3 for more details.

2.2. **Sliding vector field.** In order to compute the MSF, equations (16) and (17) only require knowledge of the sliding vector field for a single agent $\boldsymbol{z}$, $\boldsymbol{f}_\Sigma(\boldsymbol{z})$. In fact, in [13, Lemma 8, Remark 9], we derived the sliding vector field along $\boldsymbol{\Sigma}$ at synchronous points and showed (see also Theorem 2.4 below), that $\boldsymbol{F}_\Sigma(\boldsymbol{x}_s) = \boldsymbol{e} \otimes \boldsymbol{f}_\Sigma(\boldsymbol{z})$, with $\boldsymbol{e} = (1, \dots, 1)^T \in \mathbb{R}^N$. We also derived the sliding vector field at synchronous points along the $\boldsymbol{\Sigma}_i$'s since this is needed to justify the form of the saltation matrices in (17).

In the present paper, we wish to integrate the PWS network in forward time for initial conditions in a neighborhood of the synchronous periodic orbit $\boldsymbol{x}_s(t)$ in order to i) ascertain results obtained with the MSF, i.e., integrate in forward time to verify asymptotic stability or instability of $\boldsymbol{x}_s(t)$; and ii) study the transient behavior of solutions in a neighborhood of $\boldsymbol{x}_s$. Perturbations of $\boldsymbol{x}_s$ in the synchronous subspace $\mathcal{S}$ always converge to $\boldsymbol{x}_s$, hence we are interested in integrating the whole network transversally to $\mathcal{S}$. Now, while solutions in $\mathcal{S}$ can only belong to R_1, R_{2^N}, and $\boldsymbol{\Sigma}$, perturbed solutions might belong to any of the R_j's and might cross or slide along the $\boldsymbol{\Sigma}_i$'s and/or the intersection of two or more of the $\boldsymbol{\Sigma}_i$'s. In general, we can define infinitely many Filippov sliding vector fields on the intersection of two or more discontinuity surfaces. This is because the convex hull of the vector fields defined in the neighborhood of such an intersection in general contains infinitely many vectors tangent to the intersection. By Filippov construction, these tangent vectors are all feasible sliding vector fields. However, see Theorem 2.4 below; for (14), the sliding vector field on the intersection of two or more of the $\boldsymbol{\Sigma}_i$'s is always uniquely defined.

The following definitions will be handy. Let $\boldsymbol{z}_s = (\boldsymbol{z}, \dots, \boldsymbol{z})^T \in \boldsymbol{\Sigma}$ be a synchronous point on $\boldsymbol{\Sigma}$. Then, we say that $\boldsymbol{z}_s$ is a *synchronous nodally attractive sliding point* if the following conditions are verified (see (7))

$$\boldsymbol{e}_1^T \boldsymbol{f}^-(\boldsymbol{z}) > 0, \;\; \boldsymbol{e}_1^T \boldsymbol{f}^+(\boldsymbol{z}) < 0, \tag{18}$$

i.e., if $\boldsymbol{z} \in \mathbb{R}^n$ is an attractive sliding point for the single agent. It follows that $\boldsymbol{F}_j(\boldsymbol{z}_s)$ points toward $\boldsymbol{\Sigma}$ for all $j = 1, \dots, 2^N$, and solutions that reach $\boldsymbol{z}_s$ cannot leave $\boldsymbol{\Sigma}$. Similarly, we say that $\boldsymbol{z}_s$ is a *synchronous crossing point* if $\boldsymbol{z} \in \mathbb{R}^n$ is a transversal crossing point for the single agent; see (6). Solutions that reach $\boldsymbol{z}_s$ cross $\boldsymbol{\Sigma}$ into R_1, $(\boldsymbol{e}_1^T \boldsymbol{f}^-(\boldsymbol{z}) < 0)$, or into R_{2^N}, $(\boldsymbol{e}_1^T \boldsymbol{f}^-(\boldsymbol{z}) > 0)$. We say that $\boldsymbol{z}_s$ is a tangential exit point into R_1 (resp. R_{2^N}) if $\boldsymbol{z}$ is a tangential exit point into R^- (resp. R^+), see; (9).

Let C be a subset of $\{1,\dots,N\}$, and denote by $\boldsymbol{\Sigma}_C$ the intersection of the $\boldsymbol{\Sigma}_i$'s, $i \in C$. Let $\boldsymbol{y} = (\boldsymbol{y}_1,\dots,\boldsymbol{y}_N) \in \boldsymbol{\Sigma}_C$. Then, we say that $\boldsymbol{y}$ is a *nodally attractive sliding point* if all vector fields in a neighborhood of $\boldsymbol{y}$ point towards $\boldsymbol{\Sigma}_C$, Then, a solution that reaches $\boldsymbol{\Sigma}_C$ cannot leave it and starts sliding along $\boldsymbol{\Sigma}_C$. Of course, a sliding motion along $\boldsymbol{\Sigma}_C$ might take place under weaker assumptions; see Remark 2.5. However, in a neighborhood of a synchronous periodic orbit with sliding portions on $\boldsymbol{\Sigma}$, the sliding points on $\boldsymbol{\Sigma}_C$ are nodally attractive; see Remark 2.3. We say that $\boldsymbol{y}$ is a *crossing point* if $(\boldsymbol{e}_1^T\boldsymbol{f}^-(\boldsymbol{y}_i))(\boldsymbol{e}_1^T\boldsymbol{f}^+(\boldsymbol{y}_i)) > 0$ for all $i \in C$. As for tangential exit points, multiple scenarios are possible since solutions might leave $\boldsymbol{\Sigma}_C$ to slide along a lower co-dimension hyperplane or they might leave $\boldsymbol{\Sigma}_C$ to enter into one of the R_j's.

Remark 2.3. Let $\mathcal{S}$ be the synchronous subspace (3) and let $\boldsymbol{z}_s \in \boldsymbol{\Sigma}\cap\mathcal{S}$ be a synchronous nodally attractive sliding point. Then, there is a d sufficiently small such that for $\|\boldsymbol{y}-\boldsymbol{z}_s\| < d$, all vector fields $\boldsymbol{F}_j$'s, evaluated at $\boldsymbol{y}$, point toward $\boldsymbol{\Sigma}$. In particular, if $\boldsymbol{y} \in \boldsymbol{\Sigma}_C\backslash\boldsymbol{\Sigma}$, then $\boldsymbol{y}$ is a nodally attractive sliding point. Any solution of (14) through $\boldsymbol{y}$ must slide along $\boldsymbol{\Sigma}_C$ and, if $\boldsymbol{\Sigma}_C \neq \boldsymbol{\Sigma}$, the sliding motion on $\boldsymbol{\Sigma}_C$ must be toward $\boldsymbol{\Sigma}$. If $\boldsymbol{z}_s \in \boldsymbol{\Sigma}$ is a synchronous crossing point, then in a neighborhood of $\boldsymbol{z}_s$, all points $\boldsymbol{y} \in \boldsymbol{\Sigma}_C$ must be crossing points as well.

In general, the Filippov sliding vector field on the intersection of discontinuity manifolds is ambiguous; see [19, Chapter 2, Section 4]. However, when $\boldsymbol{y} \in \boldsymbol{\Sigma}_C$ is a nodally attractive point, below we show that for system (14), the intersection of $\boldsymbol{\Sigma}_C$ with the convex hull of the vector fields evaluated at $\boldsymbol{y}$ contains only one vector.

Theorem 2.4. *Let $\boldsymbol{y} = (\boldsymbol{y}_1,\dots,\boldsymbol{y}_N) \in \boldsymbol{\Sigma}_C$ be a nodally attractive sliding point. Then, there is a unique Filippov sliding vector field on $\boldsymbol{\Sigma}_C$. Moreover, if $\boldsymbol{\Sigma}_C = \boldsymbol{\Sigma}$ and $\boldsymbol{z}_s = (\boldsymbol{z},\dots,\boldsymbol{z})^T$ is synchronous, then $\boldsymbol{F}_{\boldsymbol{\Sigma}}(\boldsymbol{z}_s) = \boldsymbol{e}\otimes\boldsymbol{f}_{\Sigma}(\boldsymbol{z})$, where $\boldsymbol{e} = (1,\dots,1) \in \mathbb{R}^N$ and $\boldsymbol{f}_{\Sigma}(\boldsymbol{z})$ is the sliding vector field of (4) along Σ.*

Proof. For simplicity, we consider the case of a point $\boldsymbol{y} \in \boldsymbol{\Sigma}$, $\boldsymbol{y}$ not necessarily synchronous. The case $\boldsymbol{\Sigma}_C \neq \boldsymbol{\Sigma}$ is analogous, but the notation is cumbersome; below, we note in parentheses the required modifications. Recalling (15), in order to define the sliding vector field on $\boldsymbol{\Sigma}$, we need to consider the convex combination of all 2^N vector fields $\boldsymbol{G}_j$'s and impose tangency conditions to $\boldsymbol{\Sigma}$. (The proof for $\boldsymbol{\Sigma}_C$ requires instead the convex combination of the $\boldsymbol{G}_j$'s defined in a neighborhood of $\boldsymbol{\Sigma}_C$.) The sliding vector field along $\boldsymbol{\Sigma}$ is given by

$$\boldsymbol{F}_{\boldsymbol{\Sigma}}(\boldsymbol{y}) = \sum_{j=1}^{2^N}\lambda_j\boldsymbol{F}_j(\boldsymbol{y}) + \sum_{k=1}^{p}\sigma_k M_k\boldsymbol{y}, \tag{19}$$

and we need to impose $\lambda_j \geq 0$, $\sum_{j=1}^{2^N}\lambda_j = 1$, and the N tangency conditions to the R_i's. In general, this gives an underdetermined system and we may expect an ambiguous sliding vector field. However, for (14), the sliding vector field is uniquely defined. Indeed, the convex combination of the $\boldsymbol{F}_j$' rewrites as

$$\boldsymbol{F}_{\boldsymbol{\Sigma}}(\boldsymbol{y}) = \begin{pmatrix} (1-\mu_1)\boldsymbol{f}^-(\boldsymbol{y}_1)+\mu_1\boldsymbol{f}^+(\boldsymbol{y}_1) \\ (1-\mu_2)\boldsymbol{f}^-(\boldsymbol{y}_2)+\mu_2\boldsymbol{f}^+(\boldsymbol{y}_2) \\ \vdots \\ (1-\mu_N)\boldsymbol{f}^-(\boldsymbol{y}_N)+\mu_N\boldsymbol{f}^+(\boldsymbol{y}_N) \end{pmatrix} + \sum_{k=1}^{p}\sigma_k M_k\boldsymbol{y}, \tag{20}$$

where the μ_i's are the sum of 2^{N-1} of the λ_j's. In particular, $\mu_i = \sum_j \lambda_j$ with j is chosen such that in the sign sequence assigned to R_j there is a + in the i-th place. To illustrate, for $N = 3$, $\mu_1 = \lambda_5 + \lambda_6 + \lambda_7 + \lambda_8$, $\mu_2 = \lambda_3 + \lambda_4 + \lambda_7 + \lambda_8$, $\mu_3 = \lambda_2 + \lambda_4 + \lambda_6 + \lambda_8$.

When we impose the tangency conditions, we obtain

$$\mu_i(\boldsymbol{y}) = \frac{\boldsymbol{e}_1^T \boldsymbol{f}^-(\boldsymbol{y}_i)}{\boldsymbol{e}_1^T(\boldsymbol{f}^+(\boldsymbol{y}_i) - \boldsymbol{f}^-(\boldsymbol{y}_i))} + \frac{\boldsymbol{e}_1^T \sum_{k=1}^{p} \sigma_k \sum_{l=1}^{N} a_{jl} E_k(\boldsymbol{y}_l - \boldsymbol{y}_i)}{\boldsymbol{e}_1^T(\boldsymbol{f}^+(\boldsymbol{y}_i) - \boldsymbol{f}^-(\boldsymbol{y}_i))}, \tag{21}$$

$i = 1, \dots N$. (For $\boldsymbol{y} \in \boldsymbol{\Sigma}_C$, instead, we need to impose tangency conditions to the Σ_i', with $i \in C$.) The second part of the Theorem, the expression for $\boldsymbol{F}_{\boldsymbol{\Sigma}}$ at a synchronous point, is proven upon noticing that at a synchronous point (21), rewrites as

$$\mu_i(\boldsymbol{z}_s) = \frac{\boldsymbol{e}_1^T \boldsymbol{f}^-(\boldsymbol{z})}{\boldsymbol{e}_1^T(\boldsymbol{f}^+(\boldsymbol{z}) - \boldsymbol{f}^-(\boldsymbol{z}))}.$$

The result then follows from (8). □

Remark 2.5. Let $\boldsymbol{y} \in \boldsymbol{\Sigma}_C$ be any point on $\boldsymbol{\Sigma}_C$. Consider the linear combination of all the $\boldsymbol{G}_j$'s defined in a neighborhood of $\boldsymbol{y}$ and let $\mu_i(\boldsymbol{y})$, $i \in C$, be as in (21). If $\mu_i(\boldsymbol{y}) \in (0, 1)$, then the convex combination of the $\boldsymbol{G}_j$'s intersects $\boldsymbol{\Sigma}_C$ in one and only one vector and this allows one to define (with no ambiguity) a sliding vector field along $\boldsymbol{\Sigma}_C$. It then makes sense to call $\boldsymbol{y}$ a *sliding point*. The algebraic condition $\mu_i(\boldsymbol{y}) \in (0, 1)$, $i \in C$, is weaker then the requirement that all $\boldsymbol{G}_j$'s in a neighborhood of $\boldsymbol{y}$ point toward $\boldsymbol{\Sigma}_C$. Dynamically, we might have instances of partial sliding along some, but not all, of the $\boldsymbol{\Sigma}_i$'s, $i \in C$, toward $\boldsymbol{\Sigma}_C$. See [15] for an overview of the possible dynamics in a neighborhood of $\boldsymbol{\Sigma}_C$ in the case of an attractive co-dimension 2 hyperplane.

2.3. **Regularized vector field.** Theorem 2.4 states that sliding vector fields of (14) are uniquely defined and this in turn justifies numerical computations of solutions of (14). However, unless we are integrating for synchronous solutions, crossing or sliding along the intersection of k discontinuity manifolds requires to check more than 2^k conditions at each integration step for a k large, this becomes at the very least cumbersome and computationally expensive. For this reason, we consider an alternative approach for the numerical computation of solutions in a neighborhood of the synchronous solution $\boldsymbol{x}_s$. We define (see below) a regularized network, show that the solutions of this regularized network converge to solutions of (14), and numerically integrate the regularized smooth problem instead of (14). Beware that results on the regularized vector field are available in the literature only in the neighborhood of discontunuity hyperplanes (see [16]), hence in this section h is an hyperplane. Below, we consider a regularization of the whole network via a one-parameter family of vector fields; in Remark 2.6, we clarify why we can use a single parameter. We consider a convex combination of the 2^N vector fields with a sigmoidal function; this approach was introduced in [31] for a regularization around a co-dimension 1 discontinuity hyperplane and later in [1, 25, 17] for a regularization in the neighborhood of a co-dimension 2 discontinuity hyperplane. In the latter case, the convergence of regularized solutions to solutions of the original discontinuous system is guaranteed only under certain assumptions; see [25, 14]. Regularization techniques in the neighborhood of co-dimension k hyperplanes, $k > 2$, are not available in the literature, probably because they require restrictive assumptions in order to infer convergence, much in the same way as the difficulty to infer uniqueness of a sliding Filippov vector field on the intersection of k hyperplanes, for $k > 2$ (e.g., see [17]). In this section, we show that it is possible to define a suitable regularization of (14) and that its solutions converge to the solutions of (14).

We consider the following one-parameter family of smooth differential equations:

$$\dot{\boldsymbol{x}}_\epsilon = \boldsymbol{F}_\epsilon(\boldsymbol{x}_\epsilon)\ , \quad \boldsymbol{F}_\epsilon(\boldsymbol{x}_\epsilon) = \sum_{j=1}^{2^N} \lambda_{j,\epsilon}(\boldsymbol{x}_\epsilon) F_j(\boldsymbol{x}_\epsilon) + \sum_{k=1}^{p} \sigma_k M_k \boldsymbol{x}_\epsilon, \tag{22}$$

with $\sum_{j=1}^{2^N} \lambda_{j,\epsilon}(\boldsymbol{x}_\epsilon) = 1$ and $\lambda_{j,\epsilon}(\boldsymbol{x}_\epsilon) \geq 0$ smooth functions. Following the same reasoning that allowed us to rewrite (19) as (20), we rewrite (22) as

$$\dot{\boldsymbol{x}}_\epsilon = \boldsymbol{F}_\epsilon(\boldsymbol{x}_\epsilon) = \begin{pmatrix} (1-\mu_{1,\epsilon}(\boldsymbol{x}_\epsilon))\boldsymbol{f}^-(\boldsymbol{x}_{1,\epsilon}) + \mu_{1,\epsilon}(\boldsymbol{x}_\epsilon)\boldsymbol{f}^+(\boldsymbol{x}_{1,\epsilon}) \\ \vdots \\ (1-\mu_{N,\epsilon}(\boldsymbol{x}_\epsilon))\boldsymbol{f}^-(\boldsymbol{x}_{N,\epsilon}) + \mu_{N,\epsilon}(\boldsymbol{x}_\epsilon)\boldsymbol{f}^+(\boldsymbol{x}_{N,\epsilon}) \end{pmatrix} + \sum_{k=1}^{p} \sigma_k M_x \boldsymbol{x}_\epsilon, \tag{23}$$

where each $\mu_{i,\epsilon}(\boldsymbol{x}_\epsilon)$, $i = 1, \ldots, N$, is a linear combination of the $\lambda_{j,\epsilon}(\boldsymbol{x}_\epsilon)$'s. To illustrate, similarly to (20), for $N = 3$ we have

$$\mu_{1,\epsilon}(\boldsymbol{x}_\epsilon) = (\lambda_{5,\epsilon} + \lambda_{6,\epsilon} + \lambda_{7,\epsilon} + \lambda_{8,\epsilon})(\boldsymbol{x}_\epsilon),$$

$$\mu_{2,\epsilon}(\boldsymbol{x}_\epsilon) = (\lambda_{3,\epsilon} + \lambda_{4,\epsilon} + \lambda_{7,\epsilon} + \lambda_{8,\epsilon})(\boldsymbol{x}_\epsilon),$$

$$\mu_{3,\epsilon}(\boldsymbol{x}_\epsilon) = (\lambda_{2,\epsilon} + \lambda_{4,\epsilon} + \lambda_{6,\epsilon} + \lambda_{8,\epsilon})(\boldsymbol{x}_\epsilon).$$

Let $\boldsymbol{x}_\epsilon = (\boldsymbol{x}_{1,\epsilon}, \ldots, \boldsymbol{x}_{N,\epsilon})^T$. Since each $\mu_{i,\epsilon}$ appears only in the i-th equation, we **choose** $\mu_{i,\epsilon}(\boldsymbol{x}_\epsilon) = \varphi(\frac{h(\boldsymbol{x}_{i,\epsilon})}{\epsilon})$, with $\varphi(z) \in C^1(\mathbb{R})$ a sigmoidal function:

$$\varphi(z) = \begin{cases} 1, & z > 1 \\ 0, & z < -1 \end{cases},$$

and $\varphi'(z) > 0$ in $(-1, 1)$. Then, $\mu_{i,\epsilon}$ is just a function of $\boldsymbol{x}_{i,\epsilon}$.

Remark 2.6. Notice that $(1-\mu_{i,\epsilon}(\boldsymbol{x}_{i,\epsilon}))\boldsymbol{f}^-(\boldsymbol{x}_{i,\epsilon}) + \mu_{i,\epsilon}(\boldsymbol{x}_{i,\epsilon})\boldsymbol{f}^+(\boldsymbol{x}_{i,\epsilon})$ in (23) is a regularized vector field for the i-th single agent. Then, the regularized network (23) is equivalent to a network of regularized agents with the equation of the single agent being

$$\dot{\boldsymbol{z}}_\epsilon = (1-\mu_\epsilon(\boldsymbol{z}_\epsilon))\boldsymbol{f}^-(\boldsymbol{z}_\epsilon) + \mu_\epsilon(\boldsymbol{z}_\epsilon)\boldsymbol{f}^+(\boldsymbol{z}_\epsilon). \tag{24}$$

It follows that the use of a unique regularization parameter ϵ for each $j = 1, \ldots, N$ is justified since all agents in the network obey the same differential equation. We rewrite the differential equation for the i-th agent of (23) as $\dot{\boldsymbol{x}}_{i,\epsilon} = \boldsymbol{g}_i(\boldsymbol{x}_\epsilon)$, with

$$\boldsymbol{g}_i(\boldsymbol{x}_\epsilon) = (1-\mu_{i,\epsilon}(\boldsymbol{x}_{i,\epsilon}))\boldsymbol{f}^-(\boldsymbol{x}_{i,\epsilon}) + \mu_{i,\epsilon}(\boldsymbol{x}_{i,\epsilon})\boldsymbol{f}^+(\boldsymbol{x}_{i,\epsilon}) + \sum_{k=1}^{p} \sigma_k(\mathbf{e}_i^T L) \otimes E_k \boldsymbol{x}_\epsilon. \tag{25}$$

Remark 2.7. In the literature, it is known that under some generic assumptions (e.g., see [16, Lemma 8 and 18]), solutions of (24) converge to solutions of (4). However, unless we consider solutions in the synchronous subspace (3), this does not guarantee convergence of solutions of (23) to solutions of (14). Theorem 2.8 below addresses this concern. Its proof is based on Tikhonov's theorem (see [33] and the Appendix).

Theorem 2.8. *Let $\boldsymbol{z}$ be an asymptotically stable periodic solution of period T of the single agent and assume that $\boldsymbol{z}$ has a finite number of generic events. Let $\boldsymbol{x}_s(t) = (\boldsymbol{z}(t), \dots, \boldsymbol{z}(t))^T$ be the associate asymptotically stable synchronous periodic solution of (14) of period T, that intersects $\boldsymbol{\Sigma}$ along sliding arcs and/or at generic points. Let $d > 0$ and $\bar{\boldsymbol{x}} \in B_d(\boldsymbol{x}_s)$, i.e., $\bar{\boldsymbol{x}}$ such that $\|\bar{\boldsymbol{x}} - \boldsymbol{x}_s(t)\| < d$, for some $t \in [0, T)$. Denote by $\boldsymbol{x}_\epsilon(t)$ and $\boldsymbol{x}(t)$ the solutions of (23) and (14), respectively, with initial condition $\bar{\boldsymbol{x}}$. Then, for d sufficiently small,*

$$\lim_{\epsilon \to 0} \boldsymbol{x}_\epsilon(t) = \boldsymbol{x}(t),$$

uniformly in t on every compact interval.

Proof. In the proof, we consider, together with the sets $\boldsymbol{\Sigma}_i$, the boundary layers $\boldsymbol{\Sigma}_i^\epsilon = \{\boldsymbol{x} \in \mathbb{R}^{nN} | d(\boldsymbol{x}, \boldsymbol{\Sigma}_i) < \epsilon\}$, where ϵ is the regularization parameter used in (23), and $d(\boldsymbol{x}, \boldsymbol{\Sigma}_i)$ is the distance between $\boldsymbol{x}$ and $\boldsymbol{\Sigma}_i$. Outside the boundary layers, $\boldsymbol{F}_\epsilon(\boldsymbol{x}) = \boldsymbol{G}_j(\boldsymbol{x})$ for $\boldsymbol{x} \in R_j$. It then suffices to study the limiting behavior of $\boldsymbol{x}_\epsilon(t)$ inside the boundary layers.

Neighborhood of crossing points. First, assume that $\boldsymbol{x}_s(t)$ has only crossing points in common with $\boldsymbol{\Sigma}$. Then, portions of the solution given by $\boldsymbol{x}_s(t)$ are inside R_1 and R_{2^N}, and there are also single points on $\boldsymbol{\Sigma}$ (the crossing points). Remark 2.3 implies that for d sufficiently small, the trajectory $\boldsymbol{x}(t)$ will either cross $\boldsymbol{\Sigma}$ or it will cross more that one $\boldsymbol{\Sigma}_C$ with $C \subset \{1, 2, \dots, N\}$, to eventually enter R_1 or R_{2^N}. Moreover, it is well known that $\boldsymbol{x}(t)$ is continuous with respect to $\bar{\boldsymbol{x}}$ (see [19, Chapter 2, Section 8] for example). Convergence results in the neighborhood of crossing points are simple to obtain. For ϵ sufficiently small, they follow from the observation that $\boldsymbol{x}_\epsilon(t)$ must cross $\boldsymbol{\Sigma}_i$ and $\boldsymbol{\Sigma}_i^\epsilon$ for all $i \in C$ since $\boldsymbol{x}_\epsilon(t)$ is continuous with respect to $\bar{\boldsymbol{x}}$ and, for d sufficiently small, $\boldsymbol{e}_1^T \boldsymbol{f}^-(\boldsymbol{x}_i)$ and $\boldsymbol{e}_1^T \boldsymbol{f}^+(\boldsymbol{x}_i)$ have the same sign for all $i = 1, \dots, N$. Hence, for ϵ and d sufficiently small, $\boldsymbol{e}_1^T \boldsymbol{g}_i(\boldsymbol{x}_\epsilon)$ retains the same sign, where $\boldsymbol{g}_i(\boldsymbol{x}_\epsilon)$ is the vector field for the i-th agent defined in (25). Finally, as $\epsilon \to 0$, the time spent by $\boldsymbol{x}_\epsilon(t)$ in the boundary layer goes to zero as well. For more details, see for example [16, Lemma 8].

Neighborhood of sliding arcs on $\boldsymbol{\Sigma}$. Next, assume that $\boldsymbol{x}_s(t)$ has also sliding arcs on $\boldsymbol{\Sigma}$. For d sufficiently small, we anticipate that the trajectory $\boldsymbol{x}(t)$ will slide on some of the $\boldsymbol{\Sigma}_C$'s (with $C \neq \{1, 2, \dots, N\}$) before reaching $\boldsymbol{\Sigma}$ and start sliding along it see Remark 2.3. In what follows, we prove convergence in a neighborhood of a sliding arc on $\boldsymbol{\Sigma}$, and the proof for a sliding arc on $\boldsymbol{\Sigma}_C$ requires analogous reasonings. We denote by $[t_{in}, t_{out}]$ the time interval that the trajectory $\boldsymbol{x}(t)$ spends on $\boldsymbol{\Sigma}$, and b $\boldsymbol{x}_{in}$ and $\boldsymbol{x}_{out}$, respectively, the entry point on $\boldsymbol{\Sigma}$ and the exit point from $\boldsymbol{\Sigma}$. Since outside the boundary layer $\boldsymbol{F}_\epsilon(\boldsymbol{x})$ in (23) is equal to $\boldsymbol{G}_j(\boldsymbol{x})$ in (15) for $\boldsymbol{x} \in R_j$, $\boldsymbol{x}_\epsilon$ enters and exits the boundary layer as well, and we denote by $\boldsymbol{x}_{\epsilon,in}$ and $\boldsymbol{x}_{\epsilon,out}$ the entry and exit points. Let $t_{\epsilon,in}$ and $t_{\epsilon,out}$ be the corresponding entry and exit times. Then,

$$\lim_{\epsilon \to 0} \boldsymbol{x}_{\epsilon,in} = \boldsymbol{x}_{in}, \quad \lim_{\epsilon \to 0} t_{\epsilon,in} = t_{in}. \tag{26}$$

Now, we show uniform convergence of $\boldsymbol{x}_\epsilon$ to $\boldsymbol{x}$ in $[t_{in}, t_{out}]$ and we use Tikhonov's theorem for this purpose see [33, Chapter 10] and the Appendix below. Recall that $h_i(\boldsymbol{x}) = \boldsymbol{e}_1^T \boldsymbol{x}_i - b$, and without loss of generality, take $b = 0$. Let $\boldsymbol{x}_\epsilon = (\boldsymbol{x}_{1,\epsilon}, \dots, \boldsymbol{x}_{N,\epsilon})^T$ and use the following notation $x_{i,\epsilon}^1 = \boldsymbol{e}_1^T \boldsymbol{x}_{i,\epsilon}$; then, in (23), $\mu_{i,\epsilon}(\boldsymbol{x}_\epsilon) = \varphi(\frac{x_{i,\epsilon}^1}{\epsilon})$, and since φ is a strictly increasing function of its argument, we can express $x_{i,\epsilon}^1$ in function of $\mu_{i,\epsilon}$ and use $\mu_{i,\epsilon}$ as dependent variable instead. Then, $\frac{d\mu_{i,\epsilon}}{dt} =$

$\frac{d\mu_{i,\epsilon}}{dx^1_{i,\epsilon}}\frac{dx^1_{i,\epsilon}}{dt} = \frac{1}{\epsilon}\varphi'(\frac{x^1_{i,\epsilon}}{\epsilon})\frac{dx^1_{i,\epsilon}}{dt} = \frac{1}{\epsilon}\theta(\mu_{i,\epsilon})\frac{dx^1_{i,\epsilon}}{dt}$, with $\theta(\mu_i^\epsilon) = \varphi'(\frac{x_i^1}{\epsilon})$ and $\theta(\mu_{i,\epsilon}) > 0$. For $i = 1, \dots, N$, let $\boldsymbol{y}_{i,\epsilon} = Z\boldsymbol{x}_{i,\epsilon}$, with $Z \in \mathbb{R}^{n\times n}$, $Z = \begin{pmatrix} 0 & 0 \\ 0 & I_{n-1} \end{pmatrix}$ and rewrite (23) in the new variables $(\mu_{i,\epsilon}, \boldsymbol{y}_{i,\epsilon})$, $i = 1, \dots, N$, as

$$\begin{cases} \epsilon\dot{\mu}_{i,\epsilon} = \theta(\mu_{i,\epsilon})\boldsymbol{e}_1^T\boldsymbol{g}_i(\boldsymbol{x}_\epsilon), \\ \dot{\boldsymbol{y}}_{i,\epsilon} = Z\boldsymbol{g}_i(\boldsymbol{x}_\epsilon), \qquad i = 1, \dots, N, \end{cases} \tag{27}$$

where $\boldsymbol{g}_i(\boldsymbol{x}_\epsilon)$ is defined in (25).

The initial conditions for (27) are given at time $t = t_{in}$: $(\mu_{i,\epsilon}(t_{in}), \boldsymbol{y}_{i,\epsilon}(t_{in}))$ and they can be obtained from $\boldsymbol{x}_\epsilon(t_{in})$. In general, $\boldsymbol{x}_\epsilon(t_{in}) \neq \boldsymbol{x}_\epsilon(t_{\epsilon,in}) = \boldsymbol{x}_{\epsilon,in}$. Nonetheless, $\lim_{\epsilon\to 0} t_{\epsilon,in} = t_{in}$, together with boundedness of $\boldsymbol{F}_\epsilon$ for all $\epsilon \geq 0$, implies $\lim_{\epsilon\to 0}\boldsymbol{x}_\epsilon(t_{in}) = \boldsymbol{x}_{in}$. Setting to 0 the left-hand side in (27), we obtain the *reduced system* (see (39) in the Appendix)

$$\begin{cases} 0 = \theta(\mu_{i,0})\boldsymbol{e}_1^T\boldsymbol{g}_i(\boldsymbol{x}_0), \\ \dot{\boldsymbol{y}}_{i,0} = Z\boldsymbol{g}_i(\boldsymbol{x}_0), i = 1, \dots, N, \end{cases} \tag{28}$$

where $\boldsymbol{x}_0 = (x^1_{1,0}(\mu_{1,0}), \boldsymbol{y}_{1,0}, \dots, x^1_{N,0}(\mu_{N,0}), \boldsymbol{y}_{N,0})^T$. Since $\theta(\mu_{i,0}) > 0$, the solution of (28) must satisfy $\boldsymbol{e}_1^T\boldsymbol{g}_i(\boldsymbol{x}_0) = 0$ with $\boldsymbol{g}_i$ defined in (25). Then, the values of the $\mu_{i,0}$'s, select the sliding vector field (20) on $\boldsymbol{\Sigma}$. The initial conditions for $\boldsymbol{y}_{i,0}$ are given at $t = t_{in}$ and, due to (26), they are $\boldsymbol{y}_{i,0}(t_{in}) = Z\boldsymbol{x}_{in,i}$, with $\boldsymbol{x}_{in} = (\boldsymbol{x}_{in,1}, \dots, \boldsymbol{x}_{in,N})^T$. As for $\mu_{i,0}(t_{in})$, this is given by the solution of the nonlinear equation $\boldsymbol{e}_1^T\boldsymbol{g}_i(\boldsymbol{x}_{in}) = 0$, i.e., by (21), for $i = 1, \dots, N$. It follows that $\boldsymbol{x}_0(t)$ in (28) is equal to $\boldsymbol{x}(t)$, for $t \in [t_{in}, t_{out}]$. We then wish to show that, in the limit for $\epsilon \to 0$, solutions of (27) converge to solutions of (28). Notice that the convergence is not immediate since there is not continuous dependence of solutions of (27) on ϵ. Using the time transformation $\tau = \frac{t}{\epsilon}$ and then setting $\epsilon = 0$ in (27), we obtain the *reduced fast system* (see (40) in the Appendix)

$$\begin{cases} \mu_i' = \theta(\mu_i)\boldsymbol{e}_1^T\boldsymbol{g}_i(\boldsymbol{x}), \\ \boldsymbol{y}_i' = 0, \;\; i = 1, \dots, N, \end{cases} \tag{29}$$

where $'$ denotes derivative with respect to τ. Thus, $\boldsymbol{y}_i$ is constant. Moreover, for $\epsilon = 0$, $x_i^1 = 0$, for $i = 1, \dots, N$, and the equilibria of (29) are the parameter values μ_i in (21) that define the sliding vector field on $\boldsymbol{\Sigma}$. If we show that the equilibrium of (29) is asymptotically stable uniformly in $\boldsymbol{y}_i$, then, for d sufficiently small, the hypothesis of Tikhonov's theorem (see Theorem 4.1 in the Appendix) are satisfied, and this implies convergence of solutions of (27) to solutions of (28).

To study stability, we just need to compute the eigenvalues of the Jacobian matrix of (29) evaluated at the equilibrium. At the equilibrium, we have $\boldsymbol{e}_1^T\boldsymbol{g}_i(\boldsymbol{x}) = 0$, hence we only need to consider $\theta(\mu_i)\frac{d}{d\mu_i}\boldsymbol{e}_1^T\boldsymbol{g}_i(\boldsymbol{x})$ and the Jacobian is given by $J = D\tilde{J}$, with

$$\tilde{J} = \begin{pmatrix} -\boldsymbol{e}_1^T(\boldsymbol{f}^- - \boldsymbol{f}^+)(0, \boldsymbol{y}_{1,0}) & & \\ & \ddots & \\ & & -\boldsymbol{e}_1^T(\boldsymbol{f}^- - \boldsymbol{f}^+)(0, \boldsymbol{y}_{N,0}) \end{pmatrix},$$

and $D = \begin{pmatrix} \theta(\mu_1(0,\boldsymbol{y}_{1,0})) & & \\ & \ddots & \\ & & \theta(\mu_N(0,\boldsymbol{y}_{N,0})) \end{pmatrix}$ is a diagonal matrix with positive entries. We claim that the eigenvalues of J are negative. Remark 2.3 ensures that in a neighborhood of a synchronous nodally attractive sliding point, all vector fields must point toward $\boldsymbol{\Sigma}$. Then, for d sufficiently small, the following inequalities are satisfied for $i = 1, \dots, N$,

$$\begin{aligned} &\text{(a)} \quad \boldsymbol{e}_1^T \boldsymbol{f}^-(0,\boldsymbol{y}_{i,0}) + \sigma \boldsymbol{e}_i^T L \otimes (\boldsymbol{e}_1^T \sum \sigma_k E_k)\boldsymbol{x} > 0, \\ &\text{(b)} \quad \boldsymbol{e}_1^T f^+(0,\boldsymbol{y}_{i,0}) + \sigma \boldsymbol{e}_i^T L \otimes (\boldsymbol{e}_1^T \sum_k \sigma_k E_k)\boldsymbol{x} < 0, \end{aligned}$$

where the terms $\boldsymbol{e}_1$ in (a) and (b) have $\boldsymbol{e}_1 \in \mathbb{R}^n$, and all the terms arising from the $\boldsymbol{e}_i$, $i = 1, \dots, N$, are in $\mathbb{R}^N$. Upon subtracting (b) from (a), we obtain $\boldsymbol{e}_1^T(\boldsymbol{f}^-(0,\boldsymbol{y}_{i,0}) - \boldsymbol{f}^+(0,\boldsymbol{y}_{i,0})) > 0$, so that the diagonal elements of $\tilde{J}$, and hence the eigenvalues of J, are negative. Tikhonov's theorem then insures that for d sufficiently small.

$$\lim_{\epsilon\to 0} \boldsymbol{x}_\epsilon(t) = \boldsymbol{x}(t), \;\; t \in [t_{in}, t_{out}].$$

Notice that, while the convergence of $\mu_{i,\epsilon}$ to $\mu_{i,0}$ is not uniform in $[t_{in}, t_{out}]$ (see Theorem 4.1), $\lim_{\epsilon\to 0} x^1_{i,\epsilon} = 0$, and hence, the convergence of $\boldsymbol{x}_\epsilon$ to $\boldsymbol{x}_0$ is uniform in $[t_{in}, t_{out}]$.

Neighborhood of sliding arcs on $\boldsymbol{\Sigma}_C$. The proof is analogous to the proof of the former case. Assume that at time $t = 0$, $\boldsymbol{x}(t)$ is in R_1 or R_{2^N}. Then, without loss of generality, let $C = \{1\}$ and $Cp = \{1, 2\}$ and assume that $\boldsymbol{x}(t)$ enters Σ_1 at time t^1_{in} at $\boldsymbol{x}_{in}$ and at time t^2_{in} it enters Σ_{Cp} at x^2_{in} (see Remark 2.3). Then, we first consider equations (27) for $(\mu_{1,\epsilon}, \boldsymbol{y}_{1,\epsilon})$ only, while adding the differential equations for $\boldsymbol{x}_i$, $i = 2, \dots, N$. Reasoning as before, for d sufficiently small, $\boldsymbol{x}_\epsilon(t)$ converges to the sliding portion of $\boldsymbol{x}(t)$ along Σ_1. $\boldsymbol{x}_\epsilon(t)$ enters the boundary layer of Σ_{Cp} at time $t^2_{in,\epsilon}$ at the point $x^2_{in,\epsilon}$. It does not leave the boundary layer of Σ_1. Then, we just need to consider (27) for $i = 1, 2$, and add the differential equations for $\boldsymbol{x}_i$, $i = 3, \dots, N$. We keep augmenting (27) until $\boldsymbol{x}(t)$ enters Σ.

The statement of the theorem follows upon noticing that outside the boundary layers, $\boldsymbol{F}_\epsilon(\boldsymbol{x}) = \boldsymbol{G}_j(\boldsymbol{x})$ for $\boldsymbol{x} \in R_j$. □

2.4. **Regularized synchronous solutions.** Theorem 2.8 gives convergence of solutions of (23) to solutions of (14) in a neighborhood of an asymptotically stable periodic orbit $\boldsymbol{x}_s(t)$. In what follows, given a PWS network with an asymptotically stable synchronous periodic orbit $\boldsymbol{x}_s(t)$, we want to ascertain whether its regularization (23) has an asymptotically stable periodic orbit $\boldsymbol{x}_{\epsilon,s}(t)$ that converges to $\boldsymbol{x}_s(t)$. Below, we show that this is the case for crossing periodic orbits, i.e., for a periodic orbit with crossing points only and no sliding. In this case, the crossing synchronous solution $\boldsymbol{x}_s(t)$ can only evolve in R_1 and R_{2^N} and can only cross $\boldsymbol{\Sigma}$ and at isolated points.

Remark 2.9. In [16, Theorem 6 and Remark 15] we showed that, if the single agent (4) has an asymptotically stable crossing periodic orbit $\boldsymbol{z}(t)$ ($t \in \mathbb{R}$), then, for ϵ sufficiently small, the regularized agent (24) has an asymptotically stable periodic orbit $\boldsymbol{z}_\epsilon(t)$ that converges to $\boldsymbol{z}(t)$ as $\epsilon \to 0$. Now, if the single smooth agent (24) has an asymptotically stable periodic orbit $\boldsymbol{z}_\epsilon(t)$, then the regularized network (23) has a synchronous periodic orbit $\boldsymbol{x}_{\epsilon,s}(t) = (\boldsymbol{z}_\epsilon(t), \dots, \boldsymbol{z}_\epsilon(t))$. Further, the synchronous subspace $\mathcal{S}$ defined in (3) is invariant for (23) since it is contained in the eigenspace of M associated to the 0 eigenvalue. This last observation together with asymptotic stability of $\boldsymbol{z}_\epsilon(t)$ for the single agent implies that solutions in $\mathcal{S}$ converge to $\boldsymbol{x}_{\epsilon,s}(t)$. We need to study the behavior of perturbed solutions with initial conditions transversal to $\mathcal{S}$.

In Theorem 2.10, we prove the asymptotic stability of $\boldsymbol{x}_{\epsilon,s}(t)$ for ϵ sufficiently small. We formulate the result assuming that $\boldsymbol{x}_s(t)$ crosses $\boldsymbol{\Sigma}$ in just two points, $\boldsymbol{x}_s(\tau)$ and $\boldsymbol{x}_s(\delta)$, but the result and proof generalize immediately to a finite number of isolated crossing points.

Theorem 2.10. *Assume that $\boldsymbol{x}_s(t)$, $t \in \mathbb{R}$, is a synchronous crossing periodic orbit of (14) such that the periodic orbit $\boldsymbol{x}_s(t)$ starts at $\boldsymbol{x}_s(0)$ in R_1, crosses $\boldsymbol{\Sigma}$ at time τ at $\boldsymbol{x}_s(\tau) = (\boldsymbol{z}(\tau), \dots, \boldsymbol{z}(\tau))$ and enters R_{2^N}; then, it crosses $\boldsymbol{\Sigma}$ again at time δ at $\boldsymbol{x}_s(\delta) = (\boldsymbol{z}(\delta), \dots, \boldsymbol{z}(\delta))$ and enters in R_1 and finally at time T, $\boldsymbol{x}_s(T) = \boldsymbol{x}_s(0)$.*

If $\boldsymbol{x}_s(t)$ is asymptotically stable, then there exists $\epsilon_0 > 0$ such that (23) admits a synchronous periodic orbit $\boldsymbol{x}_{\epsilon,s}(t)$ for $\epsilon < \epsilon_0$ and such that $\lim_{\epsilon\to 0} \boldsymbol{x}_{\epsilon,s}(t) = \boldsymbol{x}_s(t)$. Moreover, $\boldsymbol{x}_{\epsilon,s}(t)$ is asymptotically stable.

Proof. The first part of the proof is in Remark 2.9. We show that $\boldsymbol{x}_{\epsilon,s}(t)$ is asymptotically stable. Let T_ϵ be the period of $\boldsymbol{x}_{\epsilon,s}(t)$. In order to study the stability properties of $\boldsymbol{x}_{\epsilon,s}(t)$, we linearize (23) along $\boldsymbol{x}_{\epsilon,s}(t)$ and consider the monodromy matrix $Y_\epsilon(T_\epsilon)$. Y_ϵ satisfies the following linearized equation

$$\dot{Y}_\epsilon = \left(I_N \otimes D\boldsymbol{f}_\epsilon(\boldsymbol{z}_\epsilon(t)) + \sum_{k=1}^{p} \sigma_k M_k \right) Y_\epsilon, \quad Y_\epsilon(0) = I_{nN}, \tag{30}$$

where $\boldsymbol{f}_\epsilon(\boldsymbol{z}_\epsilon)$ is the regularized vector field for the single agent; see (24). The monodromy matrix of (14) along $\boldsymbol{x}_s(t)$ is denoted by $Y(t)$. Then, $Y(t)$ is a piecewise continuous function with jumps at the crossing points given by saltation matrices at $\boldsymbol{x}_s(\tau)$ and $\boldsymbol{x}_s(\delta)$. That is, we can write

$$Y(T) = Y_3(T, \delta)(I_N \otimes S_{+,-})Y_2(\delta, \tau)(I_N \otimes S_{-,+})Y_1(\tau, 0), \tag{31}$$

$S_{-,+}$ and $S_{+,-}$ are the saltation matrices in (17), $\dot{Y}_1 = (I_N \otimes Df^-(\boldsymbol{z}(t)) + \sum_{k=1}^{p} \sigma_k M_k) Y_1$, $Y_1(0,0) = I_{nN}$, $\dot{Y}_2 = (I_N \otimes Df^+(\boldsymbol{z}(t)) + \sum_{k=1}^{p} \sigma_k M_k) Y_2$, $Y_2(\tau, \tau) = I_{nN}$, and $\dot{Y}_3 = (I_N \otimes Df^-(\boldsymbol{z}(t)) + \sum_{k=1}^{p} \sigma_k M_k) Y_3$, $Y_{1,3}(\delta, \delta) = I_{nN}$. The expression of the saltation matrices for the whole network as a Kronecker product of the identity matrix with the saltation matrix of the single agent has been derived in [13, Theorem 12].

Finally, we let

$$\boldsymbol{\Sigma}^- = \{\boldsymbol{x} \in \mathbb{R}^{nN} | h_i(\boldsymbol{x}) = -\epsilon, \;\; i = 1, \dots, N\},$$

$$\boldsymbol{\Sigma}^+ = \{\boldsymbol{x} \in \mathbb{R}^{nN} | h_i(\boldsymbol{x}) = \epsilon, \;\; i = 1, \dots, N\}.$$

For $Y_\epsilon(T_\epsilon)$, we have

$$Y_\epsilon(T_\epsilon) = Y_\epsilon(T_\epsilon, \delta_{2,\epsilon})Y_\epsilon(\delta_{2,\epsilon}, \delta_{1,\epsilon})Y_\epsilon(\delta_{1,\epsilon}, \tau_{2,\epsilon})Y_\epsilon(\tau_{2,\epsilon}, \tau_{1,\epsilon})Y_\epsilon(\tau_{1,\epsilon}, 0), \tag{32}$$

where by $\tau_{1,\epsilon}$ we denote the time at which $\boldsymbol{x}_\epsilon(t)$ reaches $\boldsymbol{\Sigma}^-$ from R_1 and by $\tau_{2,\epsilon}$ the time at which it reaches $\boldsymbol{\Sigma}^+$ to enter into R_{2^N}. Similarly, $\delta_{1,\epsilon}$ is the time at which $\boldsymbol{x}_\epsilon(t)$ reaches $\boldsymbol{\Sigma}^+$ from R_{2^N}, and $\delta_{2,\epsilon}$ is the time at which it reaches $\boldsymbol{\Sigma}^-$ to enter in R_1. The existence of these crossing times $\tau_{1,\epsilon}, \dots, \delta_{2,\epsilon}$, is ensured by convergence of $\boldsymbol{x}_{\epsilon,s}$ to $\boldsymbol{x}_s$ and by the following inequalities in the neighborhood of any crossing point (recall (15)):

$$(\nabla h_i^T \boldsymbol{G}_1(\boldsymbol{x}))(\nabla h_i^T \boldsymbol{G}_{2^N}(\boldsymbol{x})) > 0, \;\; (\nabla h_i^T \boldsymbol{F}_\epsilon(\boldsymbol{x}))(\nabla h_i^T \boldsymbol{G}_1(\boldsymbol{x})) > 0, i = 1, \dots, N.$$

The validity of this last expression is justified by the fact that we are linearizing along the synchronous solution, hence $\sigma M \boldsymbol{x} = 0$, and thus we just need to look at the single agent.

In a neighborhood of a crossing point, we have $\left(\nabla h_i(\boldsymbol{z})^T \boldsymbol{f}^-(\boldsymbol{z})\right)\left(\nabla h_i(\boldsymbol{z})^T \boldsymbol{f}^+(\boldsymbol{z})\right) > 0$ and, hence, the inequality above. Below we show i) convergence of $Y_\epsilon(\tau_{1,\epsilon}, 0)$ to $Y_1(\tau, 0)$, and ii) convergence of $Y_\epsilon(\tau_{2,\epsilon}, \tau_{1,\epsilon})$ to $(I_N \otimes S_{-,+})$. The convergence of the other transition matrices can be shown in a similar way.

i) Notice that $\lim_{\epsilon\to 0} \tau_{1,\epsilon} = \lim_{\epsilon\to 0} \tau_{2,\epsilon} = \tau$. Also, for ϵ sufficiently small $\tau_{1,\epsilon} < \tau$. Let $V_\epsilon(t) = Y_\epsilon(t, 0) - Y_1(t, 0)$ for $t \in [0, \tau_{1,\epsilon}]$. Then

$$\begin{cases} \dot{V}_\epsilon = (I_N \otimes D\boldsymbol{f}^-(\boldsymbol{z}(t)) + \sum_{k=1}^p \sigma_k M_k)V \\ \qquad + \left[I_N \otimes D\boldsymbol{f}_\epsilon(\boldsymbol{z}_\epsilon(t)) - I_N \otimes D\boldsymbol{f}^-(\boldsymbol{z}(t))\right] Y_\epsilon \;\; . \\ V_\epsilon(0) = 0 \end{cases}$$

Using the variation of constants formula and $V_\epsilon(0) = 0$, we obtain

$$V_\epsilon(t) = \int_0^t \left[Y_1(t,s)\left(I_N \otimes D\boldsymbol{f}_\epsilon(\boldsymbol{z}_\epsilon(s)) - I_N \otimes D\boldsymbol{f}^-(\boldsymbol{z}(s))\right) Y_\epsilon(s,0)\right] ds,$$

for $t \in [0, \tau_{1,\epsilon}]$. Since $\lim_{\epsilon\to 0} D\boldsymbol{f}_\epsilon(\boldsymbol{z}_\epsilon(s)) = D\boldsymbol{f}^-(\boldsymbol{z}(s))$ in $[0,\tau)$ and Y_ϵ bounded in $[0, \tau_{1,\epsilon}]$, it follows

$$\lim_{\epsilon\to 0} V_\epsilon(t) = \lim_{\epsilon\to 0}(Y_\epsilon(t,0) - Y_1(t,0)) = 0, \;\; t \in [0,\tau).$$

ii) Let

$$\dot{Z}_\epsilon = (I_N \otimes D\boldsymbol{f}_\epsilon(\boldsymbol{z}_\epsilon(t)))Z_\epsilon.$$

Then $Z_\epsilon(t) = I_N \otimes X_\epsilon(t)$, where by $X_\epsilon(t)$ we denote the monodromy matrix for the linearized dynamics of the regularized single agent. Moreover, $\lim_{\epsilon\to 0} Z_\epsilon(\tau_{2,\epsilon}, \tau_{1,\epsilon}) = I_N \otimes S_{-,+}$, see [16, Lemma 11]. Using the variation of constants formula, we have

$$Y_\epsilon(t, \tau_{1,\epsilon}) = Z_\epsilon(t, \tau_{1,\epsilon}) + \int_{\tau_{1,\epsilon}}^t Z_\epsilon(t,s)\left(\sum_{k=1}^p \sigma_k M_k\right) Y_\epsilon(s, \tau_{1,\epsilon}) ds, \;\; t \in (\tau_{1,\epsilon}, \tau_{2,\epsilon}).$$

Gronwall's Lemma applied to this equality insures that Y_ϵ is bounded. This together with $\lim_{\epsilon\to 0} \tau_{2,\epsilon} - \tau_{1,\epsilon} = 0$ implies that

$$\lim_{\epsilon\to 0} Y_\epsilon(\tau_{2,\epsilon}, \tau_{1,\epsilon}) = \lim_{\epsilon\to 0} Z_\epsilon(\tau_{2,\epsilon}, \tau_{1,\epsilon}) = I_N \otimes S_{-,+}. \qquad \square$$

Remark 2.11. If the PWS network has an asymptotically stable synchronous periodic orbit $\boldsymbol{x}_s(t)$ with sliding portions, we do not have a result analogous to Theorem 2.10. However, Theorem 2.8 guarantees that solutions of (23) remain in a neighborhood $B_d(\boldsymbol{x}_s)$ of $\boldsymbol{x}_s(t)$ for $d > 0$ and $\epsilon > 0$ sufficiently small.

Recap. Let us recap the main facts and results of this section.

- The regularized network (22) is equivalent to the network of regularized agents (23). We choose only one parameter ϵ and hence we have a network of identical regularized agents(Remark 2.6).

- For ϵ sufficiently small, solutions of (23) with initial conditions in a neighborhood of the synchronous periodic orbit $\boldsymbol{x}_s(t)$ converge to solutions of (14) with same initial condition (Theorem 2.8).
- If $\boldsymbol{x}_s(t)$ is an asymptotically stable crossing periodic orbit, then, for ϵ sufficiently small, (23) has a synchronous periodic orbit $\boldsymbol{x}_{\epsilon,s}(t)$ that converges to $\boldsymbol{x}_s(t)$ as $\epsilon \to 0$(Remark 2.9).
- If $\boldsymbol{x}_s(t)$ is an asymptotically stable crossing periodic orbit, then the monodromy matrix along $\boldsymbol{x}_{\epsilon,s}(t)$ converges to the monodromy matrix along $\boldsymbol{x}_s(t)$, (Theorem 2.10). It follows that for ϵ sufficiently small, $\boldsymbol{x}_{\epsilon,s}$ is asymptotically stable as well.

3. **Two examples: MSF, limit of regularized problem, convergence to the synchronous set.** We present numerical results on two examples of PWS networks; the first is with planar agent's dynamics given by (12), for which there is an attracting periodic solution with sliding regions, and the second is a modification of a problem in [22], with agent's dynamics defined in $\mathbb{R}^3$, and for which there is an attracting periodic solution with only crossing discontinuities. Relative to the two problems we consider, we have the following goals:

(i) to use the MSF to infer stability of the synchronous periodic orbits of the PWS networks, and

(ii) to confirm the results obtained via the MSF, by direct integration of the network equations in forward time.

As for point (ii), we do not integrate directly the discontinuous network for N large. This is because solutions in a neighborhood of a synchronous solution cross or slide along the intersection of $k \leq N$ discontinuity hyperplanes, and we would need to evaluate more than 2^k vector fields at the intersection, making the numerical integration particularly difficult. Instead, we integrate the regularized network (23) in forward time. Theorem 2.8 guarantees that for ϵ sufficiently small, solutions of (23) remain in a neighborhood of solutions of (14). This in turn implies that if $\boldsymbol{x}_s(t)$ is asymptotically stable, then solutions of (23) with initial conditions in a neighborhood of $\boldsymbol{x}_s(t)$ must remain sufficiently close to it for ϵ sufficiently small. Moreover, for crossing periodic orbits, Theorem 2.10 states that, if $\boldsymbol{x}_s$ is asymptotically stable, then (23) has an asymptotically stable synchronous periodic orbit in a neighborhood of $\boldsymbol{x}_s(t)$ for ϵ sufficiently small.

3.1. **Coupled PWS oscillators with sliding.** The first problem we consider is with agents given by (12) (see [21]):

$$\begin{aligned}\dot{x}_1 &= x_2\\ \dot{x}_2 &= -x_1 \mp \frac{1}{1+\gamma|x_2 - v|},\end{aligned}$$

with the minus sign if $x_2 - v > 0$ and the plus sign if $x_2 - v < 0$. In our computations, we will fix once and for all $\gamma = 3$ and $v = 0.15$, which are the values used in [21, 20, 13].

The dynamics of this single agent exhibit an asymptotically stable periodic orbit with a sliding segment on the discontinuity plane $\Sigma := \{(x_2 - v = 0\}$. Below, we have $\nabla h = \boldsymbol{e}_2$. See the Figure on the right, and note that the orbit has one entry point on Σ and one tangential exit point from Σ, and these are the only two generic events, the remaining motion being either in R^- or on Σ.

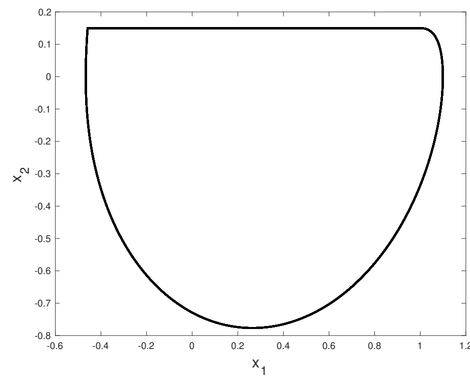

Denote the periodic solution of the single agent as $\boldsymbol{z}(t)$, so that the network (1) has a synchronous periodic solution given by $\boldsymbol{x}_s = \begin{bmatrix} \boldsymbol{z} \\ \vdots \\ \boldsymbol{z} \end{bmatrix}$. Our goal is to study the stability of this periodic orbit for the system (1) with nearest neighbor coupling; see (11) and Example 1.4.

We take two coupling matrices: $E_1 = \begin{pmatrix} 0 & 0 \\ 1 & 0 \end{pmatrix}$ as in [20] to account for elastic coupling, and $E_2 = \begin{pmatrix} 0 & 0 \\ 0 & 1 \end{pmatrix}$ to account for viscous damping. With these, the network equations are those in (10), repeated here for convenience with $\boldsymbol{f}^{\pm}$ defined in (12):

$$\begin{cases} \dot{\boldsymbol{x}}_1 & = \boldsymbol{f}^{\pm}(\boldsymbol{x}_1) + \left[\sigma_1 \begin{pmatrix} 0 & 0 \\ 1 & 0 \end{pmatrix} + \sigma_2 \begin{pmatrix} 0 & 0 \\ 0 & 1 \end{pmatrix}\right](\boldsymbol{x}_2 - \boldsymbol{x}_1), \\ \dot{\boldsymbol{x}}_i & = \boldsymbol{f}^{\pm}(\boldsymbol{x}_i) + \left[\sigma_1 \begin{pmatrix} 0 & 0 \\ 1 & 0 \end{pmatrix} + \sigma_2 \begin{pmatrix} 0 & 0 \\ 0 & 1 \end{pmatrix}\right](\boldsymbol{x}_{i+1} - 2\boldsymbol{x}_i + \boldsymbol{x}_{i-1}), \\ & \quad i = 2, \dots, N-1, \\ \dot{\boldsymbol{x}}_N & = \boldsymbol{f}^{\pm}(\boldsymbol{x}_N) + \left[\sigma_1 \begin{pmatrix} 0 & 0 \\ 1 & 0 \end{pmatrix} + \sigma_2 \begin{pmatrix} 0 & 0 \\ 0 & 1 \end{pmatrix}\right](\boldsymbol{x}_{N-1} - \boldsymbol{x}_N). \end{cases} \tag{33}$$

Now, we use the notation $\eta_1 = -\sigma_1\lambda_k > 0$, $\eta_2 = -\sigma_2\lambda_k > 0$, $k = 2, \dots, N$, where λ_k's are the eigenvalues of L (recall that for us these are all negative). With this notation, we compute the intervals in η_1 and η_2 for which the MSF is negative.

Remark 3.1. We stress that for the computation of the MSF, we do not need to take into account the number of agents. We will instead compute the largest eigenvalue in modulus of a (2×2) fundamental matrix solution (i.e., the nontrivial multiplier). When we need to find suitable values of σ_1 and σ_2 instead, we will need to account for the size of the network (hence, the eigenvalues λ_k's of L) to look for the corresponding values of $\eta_{1,2}$, which give stability (or lack thereof).

As streamlined in Section 2.1, e.g., Remark 2.2, we will need to compute the Floquet multipliers relative to the linearized problem for the single agent. In the specific situation, we recall (16) and realize that for (33), we have $(I_n + \frac{(\boldsymbol{f}^+ - \boldsymbol{f}^-)\nabla h^T}{\nabla h^T(\boldsymbol{f}^- - \boldsymbol{f}^+)}|_{\boldsymbol{z}})E_k = 0$, $k = 1, 2$. Then, we consider the following 2-dimensional linearized system (cfr.

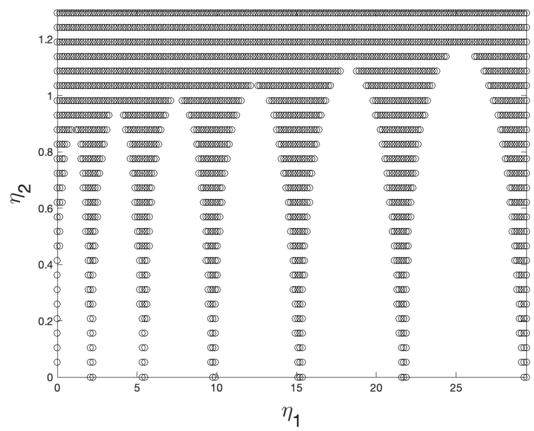

FIGURE 3. Equation (33). Stability region in function of η_1 and η_2. Dark dots indicate stability.

with [13, Equation (26)])

$$\dot{\boldsymbol{\delta}} = \begin{cases} (D\boldsymbol{f}^{\pm}(\boldsymbol{z}(t)) - \eta_1 E_1 - \eta_2 E_2)\boldsymbol{\delta}, & \boldsymbol{e}_2^T \boldsymbol{z}(t) \gtrless v, \\ D\boldsymbol{f}_{\Sigma}(\boldsymbol{z}(t))\boldsymbol{\delta}, & \boldsymbol{e}_2^T \boldsymbol{z}(t) = v, \end{cases} \tag{34}$$

and we compute the Floquet multipliers μ_1 and μ_2 along the periodic orbit $\boldsymbol{z}(t)$ in function of η_1 and η_2. Because of sliding, the saltation matrix is singular and hence, the multiplier μ_1 is always 0. When $\eta_1 = \eta_2 = 0$, (34) is the linearization along the periodic orbit of the single agent, hence $\mu_2 = 1$. In order to infer stability of the synchronous orbit $\boldsymbol{x}_s$ of the network, we look for value of η_1 and η_2 for which $|\mu_2| < 1$. In Figure 3, we show with dark circles the regions (in a portion of the (η_1, η_2)-plane) where the MSF gives stability of the synchronous solution, i.e., the values of η_1 and η_2 in (34) such that the corresponding μ_2 is less than 1 in absolute value. Quite clearly, the impact of viscous coupling is essential to obtain a stable synchronization. Moreover, synchronization is achieved for small values of η_2 when just viscous coupling is considered. To witness, in Figure 4, we plot in logarithmic scale the maximum distance between $N = 32$ oscillators, $\sigma_1 = 0$, and $\sigma_2 = 1$ for the regularized network. For the simulation, we chose $\epsilon = 0.01$ as regularization parameter and integrated the regularized network with `ode45` and `RelTol`$= 10^{-12}$. We also checked the behavior of the regularized network with both viscous and position coupling and $\sigma_1 = \sigma_2 = 1$. In this case, the network did not synchronize. This is in accordance with the synchronization region in Figure 3.

To further highlight the role of viscous damping, in Figure 5 we plot the second multiplier μ_2 in function of η_1 and η_2; on the left for elastic coupling only (matrix E_1), and on the right for viscous damping and elastic coupling with $\eta_1 = \eta_2 = \eta$. Recall that we need $|\mu_2| < 1$ to infer stability. From the computations, the coupling with $E_1 + E_2$ ensures synchronization for all values of $\eta > 1.0101$, but the results are much more restrictive for E_1 only.

In Table 1, we again consider coupling with E_1 only, and we show to which intervals η_1 must belong in order to have stable synchronization. The coupling strength

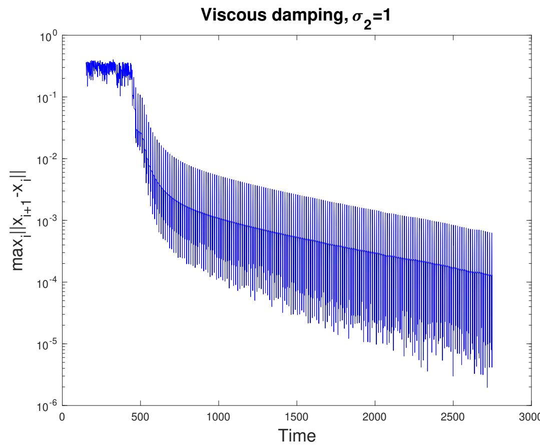

FIGURE 4. Regularization of equation (33), $\epsilon = 0.01$. Synchronization of 32 oscillators for viscous coupling.

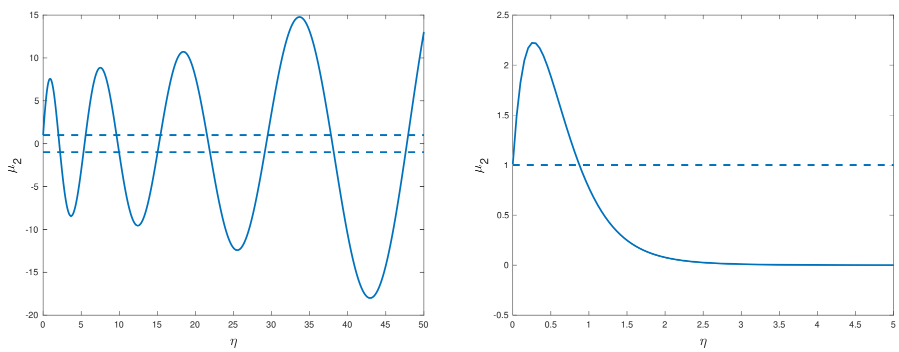

FIGURE 5. Synchronization intervals for (33) with E_1 only on the left (i.e., $\sigma_2 = 0$) and for $E_1 + E_2$ on the right.

σ_1 that insures synchronization of the N agents must be chosen so that $\sigma_1\lambda_k$ belongs to $\cup_i[\alpha_{2i+1}, \alpha_{2(i+1)}]$ for all $k = 2, \dots, N$. Using the exact eigenvalues from (11), we obtain that for $N = 2$ agents, $\lambda_2 = -2$, and hence there is synchronization for $\sigma \in \cup_{i=0}^{7}[\frac{\alpha_{2i+1}}{2} \;\; \frac{\alpha_{2(i+1)}}{2}]$. Similarly, for $N = 3$, there is synchronization for $\sigma \in [9.66 \;\; 9.81]$, while for more than 3 agents and $\sigma_1\lambda_k$ in $[0,\ 100]$, there are no synchronization intervals. As a comparison, in the case $E_1 + E_2$ (i.e., $\sigma_1 = \sigma_2 = \sigma$), the value of the coupling parameter σ that insures synchronization must be such that $\sigma\lambda_2 = \sigma(-2+2\cos(\frac{\pi}{N})) > 1.0101$; see also the right plot in Figure 5. Although this is surely feasible, for N large we would need to choose a very large coupling strength σ; see Table 2.

Remark 3.2. The distinct synchronization results for the case E_1 and the case $(E_1 + E_2)$ could be understood also by studying the behavior of the autonomous linear systems with coefficient matrices $M_1 = L \otimes E_1$ and $M_2 = L \otimes (E_1 + E_2)$, respectively The eigenvalues of the coupling matrix M_1 are all equal to 0 and defective. The corresponding linear system is then unstable. On the other hand, M_2

α_{2i+1}	$\alpha_{2(i+1)}$
2.0521	2.2022
5.3053	5.5556
9.6096	9.9600
14.9650	15.4154
21.3714	21.9219
28.9289	29.5295
37.4875	38.1882
47.1972	47.9479

TABLE 1. Equation (33). Synchronization intervals for $\sigma_2 = 0$. Values of η_1 must be in the intervals $[\alpha_{2i+1}, \alpha_{2(i+1)}]$, $i = 0, \ldots, 7$, to ensure stability of synchronous periodic orbit for just elastic coupling E_1.

N	$\sigma_{\min}$
4	1.7234
8	6.6349
16	26.2845
32	104.8850

TABLE 2. $\sigma_{\min}$ is the minimum value of σ required in order to stably synchronize N agents coupled with matrix $E_1 + E_2$.

has $(N+1)$ eigenvalues at 0 plus the $(N-1)$ eigenvalues $0 > \lambda_2 > \ldots > \lambda_N$ of the negative Laplacian matrix L. In this case, 0 is semi-simple and the linear system is dissipative. For this reason, a coupling that involves velocity (friction) is more suitable for synchronization than a coupling that involves just position.

We also investigated the behavior of two oscillators coupled by their positions only ($E = E_1$) at the bifurcation values of the parameter σ_1, for which we believe that $\sigma_1 \simeq 2.6561$ is a candidate flip bifurcation value. To see whether the two coupled oscillators undergo a period doubling bifurcation, we integrated the Filippov system in forward time for $\sigma_1 = 2.6$ and $\sigma_1 = 2.512$. Integration for the non-smooth mechanical system was done with an event location technique and a constant stepsize Runge Kutta method of order 4. In this case, we just need to check sliding/crossing/exiting on a codimension 2 discontinuity set; the number of conditions one needs to verify in this case is a doable task, and we did not need to use a regularized network. The left plot in Figure 6 is obtained for $\sigma_1 = 2.6$. After getting rid of transient, the numerical method has the invariant curve depicted

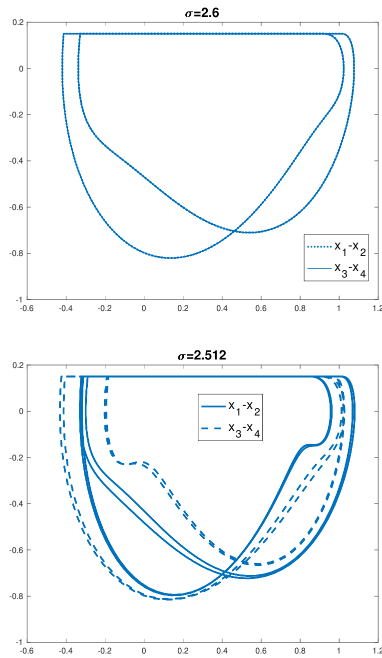

FIGURE 6. Equation (33). Numerical investigation of flip bifurcation. Left: invariant curve for two coupled oscillators and $\sigma_1 = 2.6$. The two agents are not synchronized but there is a phase shift between the two. Right: invariant curve for two coupled oscillators and $\sigma_1 = 2.512$.

in the figure, and the numerical solution is periodic of period $T \simeq 26.39$. The synchronous periodic orbit of the single agent has period $T \simeq 14.01$. We should point out that the numerical solution is not synchronous but there is a phase shift between the two masses. In the right plot, we show the invariant curve obtained for $\sigma_1 \simeq 2.512$. The numerical solution is periodic with period $T \simeq 50.61$. These numerical simulations suggest the existence of a second period doubling bifurcation of the two oscillators.

3.2. **A PWS network with crossings only.** Our second example is one of a network of piecewise linear (PWL) agents. The single agent dynamical system is given by

$$\dot{\boldsymbol{x}} = B\boldsymbol{x}\,, \quad B = \begin{cases} \begin{bmatrix} 0 & 1 & -1 \\ -1 & 1 & -1 \\ 1 & 0 & 0 \end{bmatrix}, & |x_1| < 1 \\ \\ \begin{bmatrix} 0 & 1 & -1 \\ -1 & -3/2 & -1 \\ 1 & 0 & 0 \end{bmatrix}, & |x_1| \geq 1\,. \end{cases} \tag{35}$$

The problem (35) has a periodic orbit $\boldsymbol{z}$, displayed in the figure on the right. Except for the origin and the line $\begin{bmatrix} 0 \\ t \\ t \end{bmatrix}$, which are invariant sets, this periodic solution is globally attracting in $\mathbb{R}^3$. We observe that the periodic orbit crosses the discontinuity planes $x_1 = 1, -1$ in four different locations, and there is no sliding region.

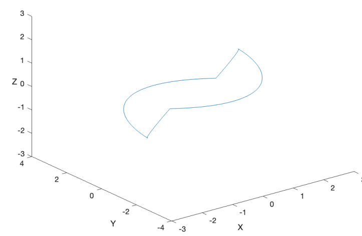

:

Our interest is in studying the stability of the synchronous periodic orbit $\boldsymbol{x}_s = \begin{bmatrix} \boldsymbol{z}(t) \\ \vdots \\ \boldsymbol{z}(t) \end{bmatrix}$ for the network (1). Here, we take the following two coupling matrices:

$$E_1 = \begin{bmatrix} 0 & 0 & 1 \\ 0 & 0 & 0 \\ 0 & 0 & 0 \end{bmatrix}, \qquad E_2 = \begin{bmatrix} 0 & 0 & 0 \\ 0 & 0 & 1 \\ 0 & 0 & 0 \end{bmatrix}, \tag{36}$$

for the Laplacian (graph) structure L given in (11). In Figure 7, we show the region, in the (η_1, η_2)-plane, where there is stable synchronization or not. Unlike the case considered in Section 3.1 (where, for sufficiently large values of the coupling parameter σ_2, the periodic orbit of (12) was always stable for the network), in the present situation for L given by (11), the MSF predicts that the synchronous solution is not going to be stable for $N = 16$, no matter the values of the two coupling parameters σ_1 and σ_2. However, for $N = 8$, there are several intervals of stability of the synchronous solution, for example for $\sigma_1 \in (1.94, 1.98)$ and $\sigma_2 \in [0, 0.04)$. To confirm this result, direct integration of the PWS network for $\sigma_1 = 1.95$ and $\sigma_2 = 0.03$, for ICs perturbed off the synchronous set by 10^{-2}, produces rather rapidly convergence to the synchronous periodic orbit; see Figure 8.

Following the same reasoning as in Remark 3.2, we also choose a second set of coupling matrices such that 0 is not a defective eigenvalue of $M = L \otimes (\sigma_1 E_1 + \sigma_2 E_2)$:

$$E_1 = \begin{bmatrix} 0 & 0 & 1 \\ 0 & 0 & 0 \\ 0 & 0 & 0 \end{bmatrix}, \qquad E_2 = \begin{bmatrix} 0 & 0 & 0 \\ 0 & 1 & 0 \\ 0 & 0 & 0 \end{bmatrix}. \tag{37}$$

Now the linear system with the coupling matrix is dissipative and we expect the network synchronization to be easier to achieve. The numerical results confirm this observation and are depicted in Figure 9.

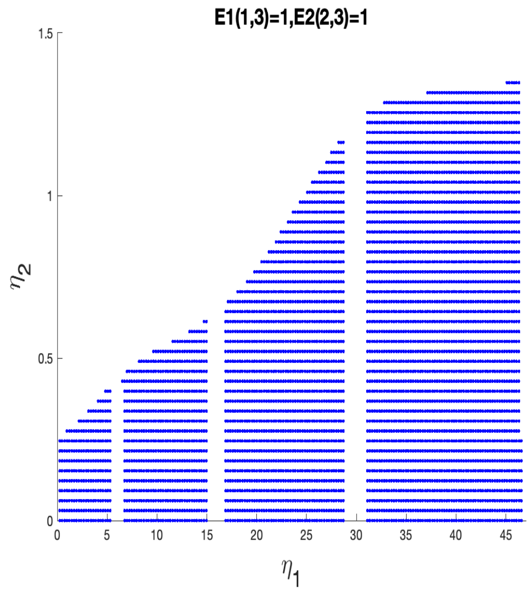

FIGURE 7. Equation (35). Synchronization region in the (η_1, η_2)-plane. There is no synchronization in the white part of the figure.

3.3. **Convergence rate to the synchronous subspace.** Whenever convergence to the synchronous subspace $\mathcal{S}$ of (3) is taking place, then we can measure the rate of attractivity to $\mathcal{S}$ by a simple numerical algorithm. The idea is that the difference between trajectories of different agents is approaching 0 at an exponential rate, which (on our two examples) we relate to the Lyapunov exponents, hence to the MSF.

For a genuine PWS system (say, like (14) with agent's vector field given by (12)), we actually apply the technique to its regularized version, so that the method below is always used on a smooth network of differential equations; see (23).

We used Algorithm 3.1 (for more than 50 different realizations of random initial conditions) on the two examples of this section, obtaining very consistent results.

- Example 3.1. We take $N = 8$, $\sigma_1 = \sigma_2 = 7$. The greatest Lyapunov exponent computed via the MSF technique (and 5 digits of accuracy) gave us $e^{-\mu_2 T} \simeq -0.0307$. Integration of the regularized network (23) with $\epsilon = 10^{-3}$, error tolerance of 10^{-10}, and using Algorithm 3.1 to estimate the convergence rate to the synchronous subspace $\mathcal{S}$ gave us $\simeq -0.032\#$, where $\# \in \{2, 3, 4\}$, which is consistent with the accuracy expected when using regularization with $\epsilon = 10^{-3}$.
- Example 3.2. Here, we do not need to regularize the system, and integrate (35) directly. We take $N = 8$, $\sigma_1 = 1.95$, and $\sigma_2 = 0.03$. Computation of the largest Lyapunov exponent with the MSF technique gives $e^{-\mu_2 T} \simeq -0.0168$, when η_j is equal to $\lambda_N \sigma_j$, $j = 1, 2$. Instead, computation of the convergence rate via Algorithm 3.1 gave us $\simeq -0.017\#$, with $\# \in \{4, 5, 6, 7\}$. As it turns

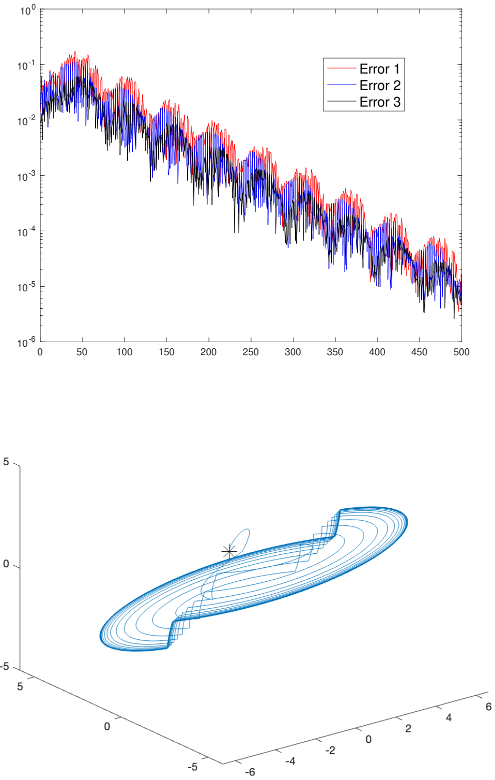

FIGURE 8. Equation (35). $N = 8$, $\sigma_1 = 1.95$, $\sigma_2 = 0.03$. Left: Convergence to synchronous periodic orbit. Right: Transient behavior and convergence for the first agent.

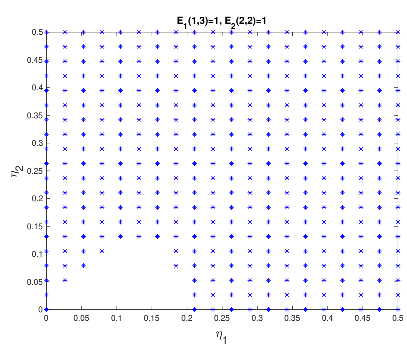

FIGURE 9. Equation (35), with matrices E_1 and E_2 as in (37), Synchronization region in the $(\eta_1 - \eta_2)$-plane. There is no synchronization in the white region on the bottom left of the figure.

Algorithm 3.1: Estimate convergence rate to $\mathcal{S}$

Input: A network differential system (2). A point $\boldsymbol{z} \in \mathcal{S}$, a value of $d > 0$ (e.g., $d = 1/10$), relative and absolute error tolerances $\texttt{Reltol}, \texttt{Abstol}$ (e.g., both equal to 10^{-10}), and an interval $[0, T_{\text{fin}}]$ (e.g., $T_{\text{fin}} = 10^3$).

Output: Convergence rate b to $\mathcal{S}$ of the trajectories of (14).

1. Integrate with an off-the-shelf integrator for the network of N agents to obtain $(t_k, \boldsymbol{x}_k)$ where $\boldsymbol{x}_k \approx \boldsymbol{x}(t_k)$.

2. Form error from synchronization at each time t_k:

$$E_k = \max_{1 \le i \le n} \max_{1 \le j \le N-1} |\boldsymbol{x}_k((j-1)n+i) - \boldsymbol{x}_k(jn+i)| \ .$$

Discard data points (t_k, E_k) as soon as they become of the same order of the error tolerances.

3. Find a least square linear fit of the data $(t_k, \ln(E_k))$ to obtain coefficients $\ln a$ and b in the exponential fit of the error ae^{bt}. The value of b is the rate of convergence to $\mathcal{S}$.

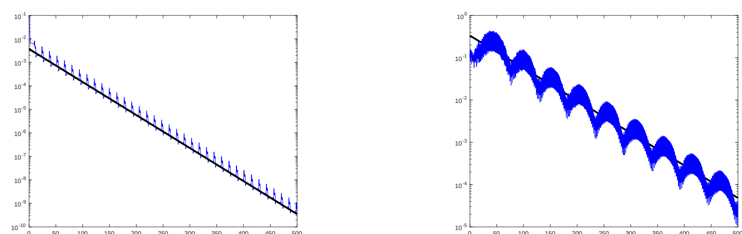

FIGURE 10. Convergence rates and line of best fit for the errors. Left: Example 3.1. Right: Example 3.2.

out, this rate is somewhere in between the values obtained from the MSF with λ_N and λ_{N-1}.

We illustrate our results by showing in Figure 10 the line of best fit, superimposed on a plot of the errors.

4. **Conclusions.** In this work, we considered networks of piecewise- smooth (PWS) differential equations with several coupling matrices, whose single agent has an asymptotically stable periodic orbit, and investigate stability of the underlying synchronous periodic orbit of the network by using both the master stability function(MSF) tool and direct integration of the *regularized network*. We proved that the solution of the regularized network converges to that of the PWS network as the regularization parameter goes to 0, and that in the case of synchronous crossing periodic orbit of the PWS network, the MSF of the regularized network converges to the MSF of the PWS network. We complemented our theoretical results with

numerical experiments on problems with synchronous periodic trajectory undergoing sliding regime or only with crossing. We also proposed a new technique to show how the convergence behavior to the synchronous subspace can be used to obtain the same rates of attractivity predicted by the MSF.

Acknowledgments. This work has been partially supported by the GNCS-Indam group and the PRIN2017, Prot. 2017E844SL research grant.

Appendix: Tikhonov theorem. Below we state Tikhonov's Theorem, Theorem 4.1. Tikhonov studied qualitative aspects of singular perturbation systems in a series of papers published in the 50's. We follow the presentation of his work in [33, Chapter 10] to state Theorem 4.1.

Consider the following Cauchy problem

$$\begin{cases} \epsilon\dot{\boldsymbol{u}}_\epsilon = \boldsymbol{f}_1(\boldsymbol{u}_\epsilon, \boldsymbol{y}_\epsilon), \\ \dot{\boldsymbol{y}}_\epsilon = \boldsymbol{f}_2(\boldsymbol{u}_\epsilon, \boldsymbol{y}_\epsilon), \\ \boldsymbol{u}_\epsilon(0) = \bar{\boldsymbol{u}}, \\ \boldsymbol{y}_\epsilon(0) = \bar{\boldsymbol{y}}. \end{cases} \tag{38}$$

with $\boldsymbol{u}_\epsilon : \mathbb{R} \to \mathbb{R}^m$, $\boldsymbol{y}_\epsilon : \mathbb{R} \to \mathbb{R}^k$ and $\epsilon \geq 0$ a given parameter. We will refer to (38) as the *full problem*. Assume $\boldsymbol{f}_1, \boldsymbol{f}_2 \in C^1(\Omega)$, with $\Omega \in \mathbb{R}^{m+k}$ open and $(\bar{\boldsymbol{u}}, \bar{\boldsymbol{y}}) \in \Omega$. Assume moreover that there exists a continuous function $\Phi : \mathbb{R}^k \to \mathbb{R}^m$ such that $\boldsymbol{f}_1(\Phi(\boldsymbol{y}), \boldsymbol{y}) = 0$. We say that $\Phi(\boldsymbol{y})$ is a root of $\boldsymbol{f}_1(\boldsymbol{u}, \boldsymbol{y})$ and we assume that it is isolated. Consider the following *reduced problem*, obtained setting $\epsilon = 0$ in (38)

$$\begin{cases} 0 = \boldsymbol{f}_1(\boldsymbol{u}_0, \boldsymbol{y}_0), \\ \dot{\boldsymbol{y}}_0 = \boldsymbol{f}_2(\boldsymbol{u}_0, \boldsymbol{y}_0), \\ \boldsymbol{u}_0(0) = \Phi(\bar{\boldsymbol{y}}), \\ \boldsymbol{y}_0(0) = \bar{\boldsymbol{y}}. \end{cases} \tag{39}$$

Notice that in (39), $\boldsymbol{u}_0(t) = \Phi(\boldsymbol{y}_0(t))$ so that $\dot{\boldsymbol{y}}_0 = \boldsymbol{f}_2(\Phi(\boldsymbol{y}_0), \boldsymbol{y}_0)$. One would like to prove that solutions of the full problem converge to solutions of the reduced problem as ϵ goes to 0, but cannot rely on continuity of solutions with respect to the parameter ϵ since the vector field in (38) is not defined for $\epsilon = 0$. Tikhonov technique uses singular perturbation theory.

Introduce the *fast time* $\tau = \frac{t}{\epsilon}$, and consider the derivative of $\boldsymbol{u}_\epsilon$ and $\boldsymbol{y}_\epsilon$ with respect to τ: $\frac{d}{d\tau} = \epsilon\frac{d}{dt}$ and denote it with $'$. We then set ϵ to 0 and obtain the following *reduced fast system*

$$\begin{cases} \boldsymbol{u}' = \boldsymbol{f}_1(\boldsymbol{u}, \boldsymbol{y}), \\ \boldsymbol{y}' = 0, \end{cases} \tag{40}$$

with initial conditions $\boldsymbol{u}(0) = \bar{\boldsymbol{u}}$ and $\boldsymbol{y}(0) = \bar{\boldsymbol{y}}$. For $\boldsymbol{y}(0) = \bar{\boldsymbol{y}}$, $\Phi(\bar{\boldsymbol{y}})$ is an isolated equilibrium of (40). Assume that there is a compact subset K of Ω such that for $(\Phi(\boldsymbol{y}), \boldsymbol{y}) \in K$, $\Phi(\boldsymbol{y})$ is an asymptotically stable equilibrium of $\boldsymbol{u}' = \boldsymbol{f}_1(\boldsymbol{u}, \boldsymbol{y})$. Under this assumption we are ready to state Tikhonov's Theorem.

Theorem 4.1. *Assume that* $\bar{\boldsymbol{u}}$ *is in the basin of attraction of the asymptotically stable equilibrium* $\Phi(\bar{\boldsymbol{y}})$ *in* (40). *Let* $T > 0$ *be such that: for every* $t \in [0, T]$, *if we let* $\widehat{\boldsymbol{y}} = \boldsymbol{y}_0(t)$, *then* $\Phi(\widehat{\boldsymbol{y}})$ *is an asymptotically stable equilibrium of* $\boldsymbol{u}' = \boldsymbol{f}_1(\boldsymbol{u}, \widehat{\boldsymbol{y}})$. *Then solutions of* (38) *converge to solutions of* (39) *as* ϵ *goes to* 0. *More specifically*

$$\lim_{\epsilon \to 0} \boldsymbol{u}_\epsilon(t) = \boldsymbol{u}_0(t) = \Phi(\boldsymbol{y}_0(t)), \text{ uniformly for } t \in (0, T]$$
$$\lim_{\epsilon \to 0} \boldsymbol{y}_\epsilon(t) = \boldsymbol{y}_0(t), \qquad \text{uniformly for } t \in [0, T].$$

We observe that the convergence of $\boldsymbol{u}_\epsilon$ cannot be uniform in $[0, T]$ since $\boldsymbol{u}_\epsilon(0) = \bar{\boldsymbol{u}} \neq \Phi(\bar{\boldsymbol{y}}) = \boldsymbol{u}_0(0)$.

REFERENCES

[1] J. C. Alexander and T. Seidman, Sliding modes in intersecting switching surfaces, I: Blending, *Houston J. Math.*, **24** (1998), 545-569.

[2] D. G. Aronson, E. J. Doedel and H. G. Othmer, An analytical and numerical study of the bifurcations in a system of linearly-coupled oscillators, *Physica D*, **25** (1987), 20-104.

[3] J. Awrejcewicz, M. Feckan and Pawel Olejnik, On continuous approximation of discontinuous systems, *Nonlinear Analysis*, **62** (2005), 1317-1331.

[4] M. Barahona and L. Pecora, Synchronization in small-world systems, *Phys. Rev. Lett.*, **89** (2002), 054101.

[5] B. K. Bera, S. Rakshit and D. Ghosh, Intralayer synchronization in neuronal multiplex network, *The European Physical Journal Special Topics*, **228** (2019), 2441–2454.

[6] K. A. Blaha, K. Huang, F. Della Rossa, L. Pecora, M. Hossein-Zadeh and F. Sorrentino, Cluster synchronization in multilayer networks: A fully analog experiment with LC oscillators with physically dissimilar coupling, *Physical Review Letters*, **122** (2019), 014101.

[7] D. A. Burbano-L., S. Yaghouti, C. Petrarca, M. de Magistris and M. di Bernardo, Synchronization in multiplex networks of Chua's circuits: Theory and experiments, *IEEE Transactions on Circuits and Systems I: Regular Papers*, **67** (2020), 927–938.

[8] S. Coombes, Y. M. Lai, M. Sayli and R. Thul, Networks of piecewise linear neural mass models, *European Journal of Applied Mathematics*, **29** (2018), 869–890.

[9] S. Coombes and R. Thul, Synchrony in networks of coupled non-smooth dynamical systems: Extending the master stability function, *European Journal of Applied Mathematics*, **27** (2016), 904–922.

[10] M. Coraggio, P. De Lellis and M. di Bernardo, Convergence and synchronization in networks of piecewise-smooth systems via distributed discontinuous coupling, *Automatica*, **129** (2021), 109596.

[11] M. Coraggio, P. De Lellis, S. J. Hogan and M. di Bernardo, Synchronization of networks of piecewise-smooth systems, *IEEE Control System Letters*, **2** (2018), 653–658.

[12] C. I. del Genio, J. Gomez-Gardenes, I. Bonamassa, and S. Boccaletti, Synchronization in networks with multiple interaction layers, *Science Advances*, **2** (2016), 1601679.

[13] L. Dieci and C. Elia, Master stability function for piecewise smooth systems, *Automatica*, **152** (2023), 110939.

[14] L. Dieci and C. Elia, Piecewise smooth systems near a co-dimension 2 discontinuity manifold: can one say what should happen?, *Discrete Contin. Dyn. Syst. Ser. S*, **9** (2016), 1039-1068.

[15] L. Dieci, C. Elia and L. Lopez, A Filippov sliding vector field on an attracting co-dimension 2 discontinuity surface, and a limited bifurcation analysis, *Journal of Differential Equations*, **254** (2013), 1800–1832.

[16] L. Dieci, C. Elia and D. Pi, Limit cycles for regularized discontinuous dynamical systems with a hyperplane of discontinuity, *Discrete Contin. Dyn. Syst. Ser. B*, **22** (2017), 3091-3112.

[17] L. Dieci and N. Guglielmi, Regularization of piecewise smooth systems, *J. Dynamics and Differential Equations*, **25** (2013), 71-94.

[18] B. Fiedler, M. Belhaq and M. Houssni, Basins of attraction in strongly damped coupled mechanical oscillators: A global example, *Zeitschrift für Angewandte Mathematik und Physik (ZAMP)*, **50** (1999), 282–300.

[19] A. F. Filippov, *Differential Equations with Discontinuous Righthand Side*, Kluwer Academic, Netherlands, 1988.

[20] U. Galvanetto and S. R. Bishop, Computational techniques for nonlinear dynamics in multiple friction oscillators, *Comput. Methods Appl. Mech. Engrg.*, **163** (1998), 373-382.

[21] U. Galvanetto, S. R. Bishop and L. Briseghella, Mechanical stick slip vibrations, *Int. Journal of Bifurcation and Chaos*, **5** (1995), 637-651.

[22] M. Itoh and L. O. Chua, Memristor oscillators, *International Journal of Bifurcation and Chaos*, **18** (2008), 3183-3206.

[23] J. Ladenbauer, J. Lehnert, H. Rankoohi, T. Dahms, E. Scholl and K Obermayer, Adaptation controls synchrony and cluster states of coupled threshold-model neurons, *Physical Review E*, **88** (2013), 042713.

[24] M. Y. Li and Z. Shuai, Global-stability problem for coupled systems of differential equations on networks, *J. of Differential Equations*, **248** (2010), 1–20.

[25] J. Llibre, P. R. da Silva and M. A. Teixeira, Study of singularities in nonsmooth dynamical systems via singular perturbation, *Siam J. Appl. Dynamical Syst.*, **8** (2009), 508–526.

[26] S. Majhi, D. Ghosh and J. Kurths, Emergence of synchronization in multiplex networks of mobile Rössler oscillators, *Physical Review E*, **99** (2019), 012308.

[27] L. Pecora and T. Carroll, Master stability functions for synchronized coupled systems, *Physical Review Letters*, **80** (1997), 2109-1112.

[28] R. Sevilla-Escoboza, I. Sendina-Nadal, I. Leyva, R. Gutierrez, J. M. Buldu and S. Boccaletti, Inter-layer synchronization in multiplex networks of identical layers, *Chaos*, **26** (2016), 065304.

[29] F. Sorrentino, Synchronization of hypernetworks of coupled dynamical systems, *New Journal of Physics*, **14** (2012), 033035.

[30] J. Sotomayor and A. L. Machado, Structurally stable discontinuous vector fields on the plane, *Qual. Theory of Dynamical Systems*, **3** (2002), 227-250.

[31] J. Sotomayor and M. A. Teixeira, Regularization of discontinuous vector fields, *International Conference on Differential Equations, Lisboa*, (1995), 207-223.

[32] L. Tang, X. Wu, J. Lü, J.-a. Lu and R. M. D'Souza, Master stability functions for complete, intralayer, and interlayer synchronization in multiplex networks of coupled Rössler oscillators, *Physical Review E*, **99** (2019), 012304.

[33] W. Wasow, Asymptotic expansions for ordinary differential equations, Dover Publications, Inc., New York, 1987.

[34] C.-W. Wu, Synchronization in dynamical systems coupled via multiple directed networks, *IEEE Transactions on Circuits and Systems-II: Express Briefs*, **68** (2021), 1660-1664.

Received February 2024; revised September 2024; early access October 2024.